Ann. Henri Poincaré *Online First*

DOI 10.1007/s00023-013-0291-3

Annales Henri Poincaré

Melons are Branched Polymers

Razvan Gurau and James P. Ryan

Abstract. Melonic graphs constitute the family of graphs arising at leading order in the $1/N$ expansion of tensor models. They were shown to lead to a continuum phase, reminiscent of branched polymers. We show here that they are in fact precisely branched polymers, that is, they possess Hausdorff dimension 2 and spectral dimension 4/3.

1. Introduction

Tensor models [1] have recently emerged as a promising conceptual and computational playground for the modern theoretical physicist. Drawing ingredients and impetuses from several topics in pure and applied mathematics, they provide a theory of random higher-dimensional spaces. More precisely, tensor models are theories of tensors in the fashion of matrix models [2], of which they may be viewed as a superset.

In particular, tensor models have been used in non-perturbative quantum gravity [3–13]. In this context, attention concentrated mostly on building models well-adapted to the problem of interest, namely a quantum theory of gravity. However, within these models, computations have been notoriously difficult to perform. There are two reasons. First, most models initially studied were highly complex, attempting to incorporate all the features developed over many years of research in the area of discrete quantum gravity [14–17]. To date, this has precluded any analysis beyond the 1st order in perturbation theory [18–21]. Second, for a long time, no generic tool existed in practice, with which to extract information about their generic features at large orders in perturbation theory.

This situation changed with the advent of what one might call modern tensor models [22]. Initially striking for their apparent simplicity, on closer inspection, they possess a rich and nuanced structure. In particular, they allow for the development of a $1/N$-expansion [23–27], that is, they come equipped with a parameter N that sensibly organizes the Feynman graphs according to

Published online: 15 December 2013

its inverse powers. In the large-N limit, one finds that only a certain subclass of graphs survive and contribute to the free energy, the melonic graphs. It is on this melonic sector that most research has concentrated, resulting in the extraction of (multi-) critical exponents [28].

These results have excited a period of high productivity, giving credence to the claim that the framework facilitates explicit calculations involving large numbers of highly refined graphs. The IID-class of models has been extended to involve matter degrees of freedom of both Ising/Potts [29] and hard dimer types [30,31], and an extensive analysis of their critical behaviours in the melonic sector has been performed. A class of dually weighted models [32] has been identified with the same melonic analysis conducted. The quantum symmetries have been formally identified [33–36] and catalogued at all orders and the resulting generators conform to a higher-dimensional Virasoro-esque Lie algebra. Indeed, there are even universality results for the critical behaviour [37]. This foundational work has influenced another concurrent line of research on tensor field theories, that is, tensor models with modified propagators that induce a renormalization group flow [38–40]. These tools may be expected to be of use in analysing the gravity-inspired models mentioned earlier [41, 42].

Intriguingly, the critical exponents extracted for the melonic sector in the plain, matter-coupled and dually weighted models are identical to those for branched polymers [43,44], which are a class of trees. Furthermore, both melonic graphs and branched polymers have spherical topology. However, while melonic graphs are reminiscent of branched polymers, these two structures are not naïvely identical. As graphs, they have markedly different connectivity and thus, need not exhibit the same intrinsic physical properties.

Fortunately, branched polymers are very well studied. After all, they have been seen to characterize phases in both euclidean and causal dynamical triangulations [45–47]. In particular, there is solid information on their Hausdorff [43] and spectral [48] dimensions, which are $d_{\mathrm{H}} = 2$ and $d_{\mathrm{S}} = 4/3$, respectively. In this paper, we show that melonic graphs have the very same Hausdorff and spectral dimensions. What is more, we claim that this conclusively identifies the class of melonic graphs as branched polymers. One might wonder why these are sufficient criteria. This stems from the fact that both the Hausdorff and spectral dimensions have a deep physical significance. The Hausdorff dimension governs the scaling of the volume with respect to the geodesic distance, while the spectral dimension is the effective dimension experienced by a diffusion process. Thus, both observables are intrinsically linked to physical processes on the structures in question.

Fortunately, we may co-opt the large body of literature on branched polymers for our own purposes. In other words, arguments translate from that case into this more general one. Having said that, certain details change upon generalization and we make efforts to highlight these clearly as we progress through the reasoning and calculations.

Two papers, in particular, have greatly influenced this work. The first [49] deals with the Hausdorff dimension of (2-dimensional) stack triangulations.

These are particular triangulations of the 2-sphere that are in correspondence with branched polymers. The authors show in particular that the Hausdorff dimension of stack triangulations equals 2. Thus, they faced an analogous problem to ours: to show that a class of objects that were, at the outset, merely in correspondence with branched polymers, truly possessed the same physical property. As a result, it was an invaluable guide through this murky terrain. The second [48] deals with the spectral dimension of branched polymers directly. Although the onus of generalization fell directly on us, this work provides both the solid background and numerous helpful insights through various technical challenges.

This paper is organized as follows: we introduce in Sect. 2 (with details and references in Appendix A) the class of melonic graphs within the tensor model setting, before proceeding to set up various correspondences to other useful classes of objects, in particular, to a class of simplicial D-balls and a class of $(D+1)$-ary trees. In Sect. 3, we construct metrics on these two classes of objects, concentrating on vertex depth, that is, the distance from a generic vertex to a distinguished root vertex. We begin Sect. 4 by showing that the depth of a randomly chosen vertex in the D-ball is, in the infinitely refined limit, a fixed rescaling of the depth of the corresponding vertex in the associated $(D+1)$-ary. This result is important for the subsequent argument (augmented by further explanation in Appendix C) pertaining to the Hausdorff dimension of the melonic D-balls. Finally, Sect. 5 deals with the spectral dimension of melonic graphs.

2. Tensor Models and Melonic Graphs

As one might imagine, tensor models are built from tensors: collections of N^D complex numbers, where N is the size of the tensor and D is the dimension, that is, the number of indices. The models themselves are a specific class of perturbed-Gaussian probability measures that are independent and identically distributed (IID) across the components of the tensor. In order to extract information about these measures, one should evaluate their partition functions and moments. Let us say a word about the partition function. For small values of the perturbation parameter, one may expand the measure as a Taylor series.[1] After evaluating the Gaussian integrals using Wick contraction, one has a sum of terms labeled by Feynman graphs. The Feynman graphs of the IID measure are bipartite edge coloured graphs, see Appendix A for more details. All the vertices of the graphs have valence $D+1$ and all the edges have a colour $0, 1$ up to D such that the $D+1$ edges incident at a vertex have distinct colours. It emerges that these terms may be organised according to the their power of $1/N$ (which is always non-negative); hence the name $1/N$-expansion. The IID measure encodes a uniform distribution over the graphs at any fixed power of $1/N$. Moreover, as $N \uparrow \infty$, only one subset of graphs survives; those for which the power of $1/N$ is zero. These graphs are known as melonic graphs,

[1] The ensuing perturbation series is not summable, but it sometimes is Borel summable [37].

a name which stems from their distinctive shape. In fact, we shall analyse the properties of a related set of graphs known as rooted melonic graphs. These are melonic graphs with one edge of colour 0 cut and they yield the 2-point function at leading order in the $1/N$-expansion.

In short, we describe the structure of rooted melonic graphs below, along with their relation to rooted $(D+1)$-ary trees, melonic D-balls and stack D-spheres. We refer the reader to Appendix A and references cited therein for details.

2.1. Connected 2-Point Function and Rooted Melonic Graphs

Rooted melonic graphs have slightly more structure than their non-rooted counterparts, are more versatile and hence prove easier on the whole to work with. They are defined in an iterative manner.

The fundamental building blocks of any rooted melonic graph are the elementary melons. Such a melon consists of two vertices connected by D edges. Both vertices have one external edge. Obviously, both external edges possess the same colour, say i (and one refers to such an object as an elementary melon of colour i). An elementary melon has two distinguished features: (i) an external edge of colour i incident to the white vertex, which is known as the root edge; (ii) $D+1$ edges incident at the black vertex, which are known as active edges, having distinct colours from $\{0, 1, \dots D\}$. The iterative definition proceeds as follows:

- $p = 1$: There is a unique rooted melonic graph with two vertices. It is illustrated in the bottom left of Fig. 1 and is the elementary melon of colour 0.
- $p = 2$: There are $D+1$ melonic graphs with four vertices. One obtains them from the graph at $p = 1$ by replacing an active edge of a given colour by an elementary melon of the same colour (as shown in Fig. 1).
- $p = k$: One obtains these graphs from those at $p = k-1$ by replacing some active edge by an elementary melon of the appropriate colour.

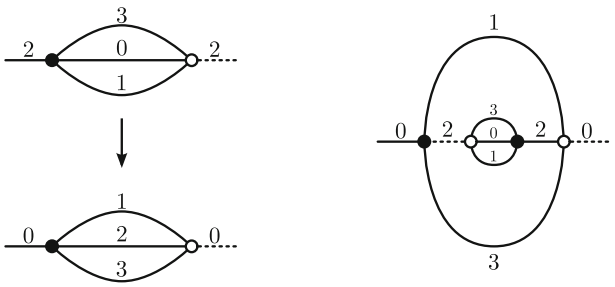

FIGURE 1. An elementary melon of color 2 inserted along the active edge of color 2 (for $D = 3$). The active edges are drawn using *full lines*

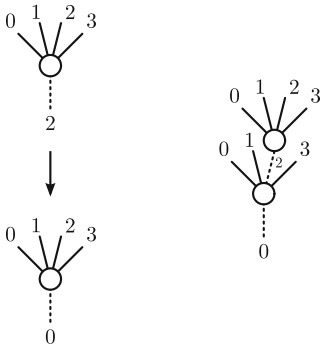

FIGURE 2. The elementary vertex of color 2 replacing a leaf of color 2 (for $D = 3$)

2.2. The Many Guises of Rooted Melonic Graphs

As mentioned earlier, the abstract structure of rooted melonic graphs coincides with that of several other objects, which we shall describe presently.

2.2.1. Colored Rooted $(D + 1)$-ary Trees. There is a simple bijection between the set of rooted melonic graphs and coloured rooted $(D + 1)$-ary trees. The fundamental building blocks of any coloured rooted $(D + 1)$-ary tree are the elementary vertices. An elementary vertex of colour i is $(D + 2)$-valent with two distinguished features: (i) a root edge of colour i; (ii) $D + 1$ active leaves each with a distinct colour from $\{0, \ldots, D\}$. These correspond to the root edge and the active edges of the elementary melon, respectively. Since this class of trees is also constructed in an iterative manner, the map is self-evident:

- $p = 1$: There is a unique coloured rooted $(D+1)$-ary tree with a single elementary vertex. This is the elementary vertex of colour 0. It is illustrated in the bottom left of Fig. 2.
- $p = 2$: There are $D+1$ such trees with two elementary vertices. One obtains them from the tree at $p = 1$ by replacing a leaf of a given colour with an elementary vertex of the same colour (as shown in Fig. 2).
- $p = k$: One obtains these trees from those at $p = k - 1$ by replacing a leaf with an elementary vertex of the same colour.

2.2.2. Coloured Simplicial D-Balls. The description of how any given $(D+1)$-coloured graph is dual, in a precise topological sense, to a unique D-dimensional abstract simplicial pseudomanifold is provided in all its detail in many contexts [50,51] (see [52,53] for a modern description). We give a heuristic summary here.

Consider first a closed $(D + 1)$-coloured graph. One identifies the set $\mathcal{B}^{(i_1 \ldots i_k)}$ of all maximally connected subgraphs with k distinct colours $\{i_1, \ldots, i_k\}$ drawn from $\{0, \ldots, D\}$. These are known as the k-bubbles of species $(i_1, \ldots, i_k)$. Note that these bubbles have a nested structure in that

k-bubbles lie nested within $(k+1)$-bubbles, which in turn lie nested within $(k+2)$-bubbles and so on.

The dual map associates a $(D-k)$-simplex with each k-bubble and the nested structure of the bubbles encodes the gluing relations of the simplices to form a unique simplicial complex. These $(D-k)$-simplices inherit the colouring of their corresponding k-bubble. Note that the vertices (0-simplices) of the dual simplicial complex are one to one to the subgraphs with D colours. The vertices are thus coloured by D colours $\{i_1, \dots i_D\}$. Alternatively, one can colour them by an unique colour: the complementary colour of their dual subgraph, $\{0, \dots D\} \backslash \{i_1, \dots i_D\}$.

Consider cutting a closed $(D+1)$-coloured graph along one edge. This results in an open graph whose dual is a simplicial complex with boundary. This boundary is a $(D-1)$-sphere constructed from two $(D-1)$-simplices.

Melonic graphs are dual to simplicial D-spheres. Rooted melonic graphs, which are melonic graphs with one edge cut, are dual to simplicial D-balls with the boundary mentioned above. For the want of a better name, we shall call them melonic D-balls. One can define them iteratively. The fundamental building blocks are the elementary melonic D-balls. These consist of two D-simplices sharing D of their $(D-1)$-simplices. There are two more $(D-1)$-simplices forming the boundary $(D-1)$-sphere. In the manner outlined above, the two D-simplices are dual to the two vertices of the elementary melon, while the $(D-1)$-simplices are dual to the edges. Thus, the $(D-1)$-simplices inherit a single colour. An elementary melonic D-ball of colour i has two distinguished features: (i) an external root $(D-1)$-simplex of colour i; (ii) $D+1$ active $(D-1)$-simplices (one of which is on the boundary), each with a distinct colour. The iterative definition proceeds as follows:

- $p=1$: There is a unique D-ball comprised of two D-simplices. It is the elementary melonic D-ball of colour 0. It is illustrated in the bottom left of Fig. 3.
- $p=2$: There are $D+1$ melonic D-balls with four D-simplices. One obtains them from the melonic D-ball at $p=1$ by adding an elementary melonic D-ball of a given colour (shown in Fig. 3). More precisely, one splits the melonic D-ball arising at $p=1$ along an active $(D-1)$-simplex (or one selects the active boundary $(D-1)$-simplex). One then glues an elementary melonic D-ball of the appropriate colour along the split (or simply on the boundary $(D-1)$-simplex).
- $p=k$: One obtains them from those at $p=k-1$ by adding an elementary melonic D-ball at some active $(D-1)$-simplex.

2.2.3. Colored Stack Simplicial D-Spheres. There is also a slightly more convoluted map between the set of coloured rooted $(D+1)$-ary trees and coloured stack simplicial D-spheres (abbreviated here to stack spheres). Stack spheres are triangulations of the D-sphere. The fundamental building blocks are the elementary stack spheres. Such an object is comprised of the $D+2$ D-simplices forming the boundary of a $(D+1)$-simplex. An elementary stack sphere of colour i has two distinguishing features: (i) it has a root D-simplex of colour i;

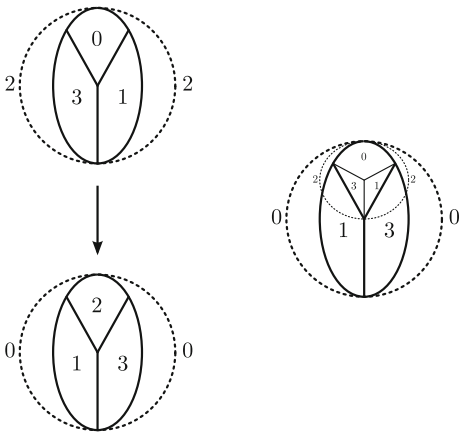

FIGURE 3. The melonic D-ball at $p = 2$ (for $D = 3$), obtained by adding an elementary D-ball of color 2

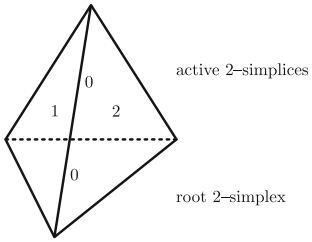

FIGURE 4. The unique stack D-sphere at $p = 1$ (for $D = 2$)

(ii) $D+1$ distinctly coloured active D-simplices drawn from $\{0, \ldots, D\}$. Moreover, there is a single vertex which is shared by all $D + 1$ active D-simplices, which we shall refer to as its active vertex. An example is illustrated in Fig. 4.

From this colouring of the D-simplices, one can colour the vertices in the following manner: the root D-simplex of colour i contains $D + 1$ of the $D + 2$ vertices. Consider such a vertex. There is a unique active D-simplex, within which it is not contained. It is labeled by the colour of that D-simplex. The final vertex (the active vertex) is not labeled by a unique colour but rather by all colours. Better said, the colour of this vertex depends on the active D-simplex, within which one is considers it, and one labels it by the colour of this D-simplex. One notes that for any given D-simplex in the elementary stack sphere, its $D + 1$ vertices are distinctly coloured. This colouring procedure is illustrated in Fig. 5.

$p = 1$: There is a the unique stack sphere comprising of $D + 2D$-simplices. It is the elementary stack sphere of colour 0.

$p = 2$: There are $D+1$ stack spheres with $2D+2D$-simplices. One obtains them from the stack sphere at $p = 1$ by constructing the connected sum

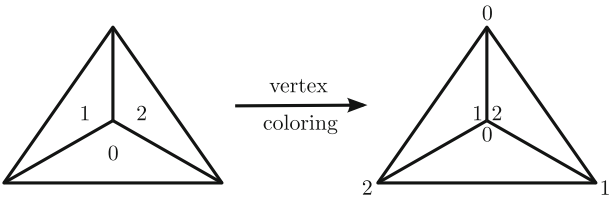

FIGURE 5. Coloring the vertices of the elementary stack sphere (for $D = 2$). Only the active 2-simplices are drawn

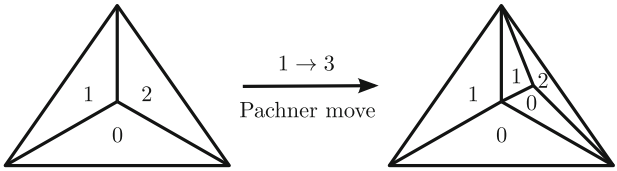

FIGURE 6. The $1 \to (D+1)$ Pachner move performed on the active D-simplex of color 2 (for $D = 2$)

of this stack sphere with an elementary stack sphere of some colour. To be more precise, one takes the stack sphere at $p = 1$ and excises an active D-simplex of some colour, say i. Having done that, one removes the root D-simplex from an elementary stack sphere of colour i. One glues the resulting D-balls together by identifying their boundaries, such that the colours of their respective boundary vertices match and the result is a D-sphere. Note that this is akin to performing a $1 \to (D+1)$ Pachner move on the active D-simplex with precisely inherited colour information. This process is drawn in Fig. 6.

$p = k$: One obtains these stack triangulations (which have $Dk + 2D$-simplices) from those at $p = k - 1$ by performing a $1 \to (D+1)$ Pachner move on an active D-simplex.

2.2.4. Words on Trees. In principle, the vertices of a coloured rooted $(D+1)$-ary tree are of two types. There are univalent vertices, at which the leaves and root edge of the tree are incident. These vertices are disregarded from now on. Rather, one concentrates on the $(D+2)$-valent vertices, to which we shall continue to refer as elementary vertices. Each tree also has a distinguished elementary vertex known as its root vertex.

Every elementary vertex of a coloured rooted $(D+1)$-ary tree has an associated word composed from the alphabet $\Sigma_D = \{0, 1, \ldots, D\}$. For a given vertex, its word is constructed by listing (left to right) all the colours one encounters on the branches, when going from the root vertex to the vertex in question. Thus, the word associated with the root vertex is ( ). An example of a generic word is given by (10132120312). This word is the canonical label discussed in [28]. It will serve our purposes better to attach to the vertices, this word supplemented by an initial letter 0, which signifies the initial root

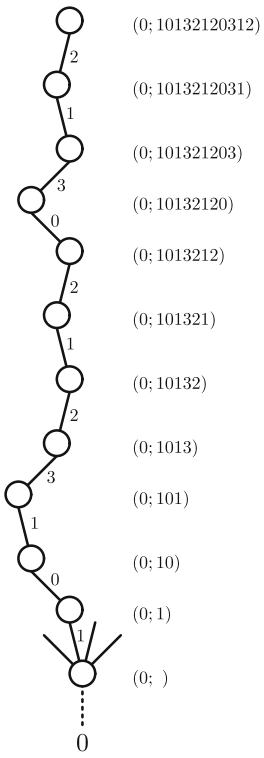

FIGURE 7. The words associated to some vertices of a colored rooted $(D+1)$-ary tree

edge of colour 0. Thus, the label of the root vertex becomes $(0;\ )$, while the sample word given a moment ago becomes $(0; 10132120312)$. This example is drawn in Fig. 7.

2.2.5. More Remarks on Vertices in Trees, Balls and Stack Spheres. At order $p = k$, a rooted melonic graph has $2k$ internal vertices, the associated coloured rooted $(D+1)$-ary tree has k elementary vertices, the associated melonic D-ball has k internal vertices, while the associated stack D-sphere has k active vertices. We shall discard any adjectives from now on and refer to these nodes simply as the vertices.

There is a clearcut correspondence between the vertices of the melonic D-ball and the vertices of the $(D+1)$-ary tree. Both the D-ball and the $(D+1)$-ary tree are generated iteratively with a single vertex added at each iteration. Moreover, both have a distinguished initial vertex called the root vertex. As mentioned already, in the $(D+1)$-ary tree, it is the vertex labeled by the word $(0;\ )$. In the D-ball, it is the corresponding vertex, which is of colour 0 and denoted by v_0.

In the same fashion, there is a correspondence between the vertices of the $(D+1)$-ary tree and the vertices of the associated stack D-sphere. For

completeness, there is a two-one correspondence between the vertices of the $(D+1)$-ary tree and the associated rooted melonic graph; each vertex of the tree is associated to an elementary melon, which in turn has two vertices.

3. Distance and Depth

3.1. Distance

For any connected graph, there is an elementary definition for the graph distance $d(v_s, v_t)$ between two vertices v_s and v_t as the minimal number edges in any contiguous path journeying from v_s to v_t.

In this case, there are four related graphical structures: a rooted melonic graph, a coloured rooted $(D+1)$-ary tree, a melonic D-ball and a stack D-sphere. Although their vertices correspond in the manner detailed above, they have different graph connectivities. Therefore, the distance between a pair of vertices in the $(D+1)$-ary tree differs in general from the distance between their corresponding vertices in the melonic D-ball and so forth.

3.2. Depth

In Sect. 2.2.4, we distinguished the vertex at the base of a $(D+1)$-ary tree as the root vertex. There are corresponding root vertices in both the associated melonic D-ball and stack D-sphere. We are interested in calculating the graph distance of a vertex from the root vertex.

The term tree depth d_{T} shall refer to the graph distance of a vertex from the root in the $(D+1)$-ary tree. In passing, this is rather simple to calculate since there is a unique path from the root to any given vertex. As mentioned above, to each vertex of a tree, there is an associated word, for example, $(0; 10132120312)$. The letters to the right of the semi-colon are exactly the edges of the tree joining the vertex to the root. Thus, one may calculate the tree depth of this vertex by counting the number of letters after the semi-colon; $d_T(0; 10132120312) = 11$.

The term depth d shall refer to the graph distance of a vertex from the root in the melonic D-ball, while the the term stack depth shall refer to the graph distance of a vertex from the root in the stack D-sphere.

Having already demonstrated how to calculate the tree depth, we shall detail here the corresponding procedure for the depth in the melonic D-ball. For the stack depth, we refer the reader to [49]. There are four parts: first, we give just a blind statement of the mechanism by which one constructs the depth; second, we provide a worked example; third, we explain the mechanism in more detail and; fourth, we describe a shorter method to calculating the depth for any given word.

3.2.1. Construction. As stated many times already, to each vertex of the melonic D-ball, there is a corresponding vertex in the associated $(D+1)$-ary tree. Thus, each vertex in the melonic D-ball is labeled by a word, for example, $(0; 10132120312)$. It emerges that one may calculate the depth of a vertex in the melonic D-ball using the associated word. The key object is the distance

array associated with that vertex, an array with $D+1$ entries that may be constructed directly from its word. It is from this distance array that the depth of the vertex in question is extracted.

To be clear at the outset, the aim of the game is to construct the depth of a vertex in a melonic D-ball. However, one first considers the associated $(D+1)$-ary tree and the corresponding vertex v_n. Assume that for this vertex, the tree depth is $d_{\mathrm{T}}(v_n) = n$. Thus, the associated word to this vertex is of the form: $w_n = (0; u_1 \dots u_n)$, where u_i are letters drawn from the alphabet $\Sigma_{D+1} = \{0, \dots, D\}$. In the tree, there is a unique path, of length n, from the root vertex to v_n. Let us denote the root vertex by v_0. This path comprises of a sequence of $n+1$ vertices marked v_i, such that $0 \leq i \leq n$. The word labelling the root vertex v_0 is $w_0 = (0; \,)$, while the word labelling v_i is just w_n with the sub-word $u_{i+1} \dots u_n$ removed, that is, $w_i = (0; u_1 \dots u_i)$. Moreover, given that one has a sequence of vertices in the $(D+1)$-ary tree, one also has a corresponding sequence of vertices in the melonic D-ball which inherit the names v_i.

One constructs the distance array associated with v_i iteratively from the words w_j, with $0 \leq j \leq i$. At the outset, one is given that the distance array associated with v_0 is $\mathfrak{da}(v_0) = (0, 1, \dots, 1)$, that is, zero followed by D ones. Now, let us assume that the distance array associated with v_i is $\mathfrak{da}(v_i) = (m_0, \dots, m_D)$ and that $u_{i+1} = j$. Then, the distance array associated to v_{i+1} is

$$\mathfrak{da}(v_{i+1}) = (m_0, \dots, m_{j-1}, \min_{k \neq j}(m_k) + 1\,, m_{j+1}, \dots, m_D). \tag{1}$$

In this manner, one can construct the distance array associated with all the v_i in the sequence.

Say that $u_i = j$ and that for v_i, the distance array is $\mathfrak{da}(v_i) = (m_0, \dots, m_j, \dots, m_D)$. The depth of v_i in the melonic D-ball is $d(v_i) = m_j$.

3.2.2. Worked Example. We consider our favorite example, a vertex v labelled by the word $w = (0; 10132120312)$.

3.2.3. Explanation. Consider the sequence of vertices v_i $(0 \leq i \leq n)$ in the melonic D-ball such that the word associated with v_i is $w_i = (0; u_1 \dots u_i)$. This sequence is generated in the following manner: one starts with initial elementary D-ball of colour 0 and adds in sequence elementary D-balls of colours u_i, for $0 \leq i \leq n$. In terms of the 1-skeleton of the melonic D-ball, adding the elementary D-ball of colour u_i entails adding the vertex v_i (of colour u_i) and joining it to D vertices (already present) labelled by distinct colours from the set $\{0, 1, \dots D\} \backslash \{u_i\}$. This action distinguishes $D+1$ vertices in the melonic D-ball. One defines the distance array associated with v_i as the array with $D+1$ entries comprised of the depths of these $D+1$ vertices, ordered according to their colour.

Consider the initial elementary D-ball of colour 0. This has a unique internal vertex of colour 0, which is the root vertex v_0. It also has D boundary vertices labelled by distinct colours from the set $\{1, 2, \dots D\}$. The word associated with the root vertex is $w_0 = (0; \,)$, while we stated that the distance

array is $\mathfrak{da}(v_0) = (0, 1, \ldots, 1)$. This encodes that the fact that the root vertex (of colour 0) is of depth 0, while the D boundary vertices are all of depth 1. Note that one knows the depth of all vertices in this melonic D-ball.

Now, consider the point where one has added the elementary D-balls in the sequence up to some point i. Assume that the distance array of v_i is $\mathfrak{da}(v_i) = (m_0, \ldots, m_D)$. According to the above definition, this encodes the depths of $D+1$ vertices in the melonic D-ball: the vertex v_i along with the D vertices to which it is connected. Within this set of vertices, one denotes momentarily the vertex with depth m_k by V_k. Now, one adds the elementary D-ball of colour $j = u_{i+1}$. At the level of the 1-skeleton, this corresponds to adding the vertex v_{i+1} of colour j and connecting it to D vertices labelled by distinct colours from the set $\{0, 1, \ldots D\}\backslash\{j\}$. By direct inspection, the vertex v_{i+1} is joined to D of the vertices V_k, that is, all except V_j. This means that all entries except the jth entry of $\mathfrak{da}(v_{i+1})$ coincide with those entries in $\mathfrak{da}(v_i)$. Moreover, any path joining v_{i+1} to the root vertex must pass through at least one of these vertices V_k. Thus, the jth entry is (1 + the minimum of the depths of the vertices V_k with $k \neq j$).

3.2.4. Calculation Via Sub-Words. Despite this iterative calculation via a distance array, there is a yet more succinct method, which shall play an active role later.

Let us denote by W_{D+1} the set of words containing all the letters of the alphabet $\Sigma_{D+1} = \{0, 1, \ldots D\}$. Consider a vertex v labelled by the word $w = (0; u_1 u_2 \ldots u_n)$. The depth of v corresponds to division of w into disjoint adjacent sub-words τ_r, comprised of letters of depth r. Thus, $\tau_0 = 0$. Then, $\tau_1 = u_1 \ldots u_{a_1}$, with $u_1, u_2, \ldots u_{a_1} \neq 0$ and $u_{a_1+1} = 0$. Furthermore, τ_r, for $r > 1$, may be one of two forms: (i) $\tau_r = u_{a_{r-1}+1} \ldots u_{a_r}$ such that $\tau_r \notin W_{D+1}$ but $\tau_r u_{a_r+1} \in W_{D+1}$; (ii) $\tau_r = u_{a_{r-1}+1} \ldots u_n$ if $u_{a_{r-1}+1} \ldots u_n \notin W_{D+1}$. This second possibility accounts for the fact that the last subword might be incomplete.

The depth of a vertex v with with word $w = \tau_0 \tau_1 \ldots \tau_k$, is

$$\Lambda(w) = d(v) = k. \tag{2}$$

As an example, take the $(3+1)$-ary tree illustrated in Figs. 7 and 8. We have listed the depth and array labels of all the vertices in the unique path from the root vertex to the vertex with label $(0; 10132120312)$. The vertical dividers highlight those letters of the word at which the depth increases.

w	0	1	0	1	3	2	1	2	0	3	1	2
$d(\cdot)$	0	1	2	2	2	3	3	3	3	4	4	4
$\mathfrak{da}(\cdot)$	$\begin{pmatrix}\mathbf{0}\\1\\1\\1\end{pmatrix}$	$\begin{pmatrix}0\\\mathbf{1}\\1\\1\end{pmatrix}$	$\begin{pmatrix}\mathbf{2}\\1\\1\\1\end{pmatrix}$	$\begin{pmatrix}2\\\mathbf{2}\\1\\1\end{pmatrix}$	$\begin{pmatrix}2\\2\\1\\\mathbf{2}\end{pmatrix}$	$\begin{pmatrix}2\\2\\\mathbf{3}\\2\end{pmatrix}$	$\begin{pmatrix}2\\\mathbf{3}\\3\\2\end{pmatrix}$	$\begin{pmatrix}2\\3\\\mathbf{3}\\2\end{pmatrix}$	$\begin{pmatrix}\mathbf{3}\\3\\3\\2\end{pmatrix}$	$\begin{pmatrix}3\\3\\3\\\mathbf{4}\end{pmatrix}$	$\begin{pmatrix}3\\\mathbf{4}\\3\\4\end{pmatrix}$	$\begin{pmatrix}3\\4\\\mathbf{4}\\4\end{pmatrix}$

FIGURE 8. Calculation of distance array and depth

To track the way in which the depth is updated from left to right, one notes that as long as one does not encounter a second letter 0, the array label remains $(0, 1, \ldots, 1)$. Hence, the depth is 1. The depth increases to 2 at the second occurrence of the letter 0 (that is the first occurrence of 0 after the semi-column) and the array label of this vertex is $(2, 1, \ldots 1)$. Then, starting from this 0, the first occurrence of a letter j shifts m_j in the array label from 1 to 2. A subsequent occurrence of the letter j has no effect on the array. At this point, as long as there are at least two entries in the array label that equal 1, the depth of the corresponding vertices remains 2. The depth increases to 3 only when the array has (i) a unique entry $m_j = 1$, (ii) $m_i = 2$ for all $i \neq j$ and (iii) the letter one encounters is j. In this instance, the array label becomes $m_j = 3$ along with $m_i = 2$ for $i \neq j$. This occurs when, starting from the second 0, one has encountered (at least once) all the letters of the alphabet. Note that, very importantly, the depth changes exactly when one encounters for the first time all the letters in the alphabet, that is, the depth of $(0; 10132)$ is 3. Using the same argument, the depth changes to 4 when, starting from the first letter of depth 3 (which in this case is 2), one has encountered again (at least once) all the letters of the alphabet, hence at $(0; 101321203)$.

The division in sub-words goes as follows:

$$w = (0; 10132120312) = (0)(1)(013)(2120)(312) \tag{3}$$

Remark on Comparison to Stack Depth: Note that the depth defined here is different from the stack depth (very similarly) defined in [49] for $D = 2$. The following is a convincing example. (In order to compare the two distances more readily, we consider a $(2 + 1)$-coloured model, such that the words are comprised of letters from the alphabet $\{1, 2, 3\}$ and the first letter 1. In other words, $u = (1; u_1 \ldots u_n)$.)

Word	1	3	1	2	3	1	2	3	1	2	3	1	2	3	1	2	3	1	2	3
Depth	0	1	2	2	3	3	4	4	5	5	6	6	7	7	8	8	9	9	10	10
Stack depth	0	1	2	2	2	3	3	3	4	4	4	5	5	5	6	6	6	7	7	7

In principle, a lot of the same structures arise in both definitions. Both depths are constructed from the words attached to the vertices of coloured rooted $(2 + 1)$-ary trees. While the depth defined here measures the distance of some vertex from the root vertex in the associated melonic 2-ball, the Albenque–Marckert depth [49] measures the distance of the vertex from the root vertex in the associated stack 2-sphere. Since the connectivity of a melonic 2-ball differs from that of its corresponding stack 2-sphere, one should not be surprised that the depths differ. Starting from the word attached to a vertex of the tree, the procedure to calculate the stack depth of the associated vertex in the stack 2-sphere is almost identical to that utilized here to calculate the depth of the associated vertex in the melonic 2-ball. As one might expect, one defines and updates a(n analogous) distance array and ultimately reads off the stack depth. The only difference is that the stack depth gets updated after one has encountered for the first time all the letters in the alphabet. Thus the stack depth lags behind the depth in the melonic D-ball.

4. Hausdorff Dimension

For a metric space X, the Hausdorff dimension d_{H} captures how the volume of a ball scales with respect to its geodesic distance. More formally defined as

$$d_{\mathrm{H}} = \inf\{d \geq 0 : \mathcal{H}_d(X) = 0\}, \tag{4}$$

where $\mathcal{H}_d(X)$ is the d-dimensional Hausdorff measure on X, that is,

$$\mathcal{H}_d(X) = \inf\left\{\delta = \sum_i r_i^d \ : \text{ the indexed collection of balls of radius } r_i \text{ cover } X\right\}. \tag{5}$$

Obviously, for the simple example of flat D-dimensional Euclidean space: $V_D \sim r^D$. Thus

$$d_{\mathrm{H}} = D. \tag{6}$$

It is clear, however, that some work must be done to extract this dimension for the class of melonic D-balls. One may follow the argument in [49], which successfully navigates this ground for the 2-dimensional case, that is, melonic 2-balls (or rather stack 2-spheres). A complete statement of their argument would be a rather laborious task and would, for the most part, amount to a literal restatement. There are, however, some points where our D-dimensional argument differs from their 2-dimensional one, summarized by the fact that we analyse melonic D-balls rather than stack D-spheres and thus utilize the depth rather than the stack depth. This motivates Lemmas 1 and 2 below. Apart from dwelling on this important technicality, we content ourselves with a descriptive account of the main theorem, which offers as a by-product the Hausdorff dimension. Some more details are given in Appendix C.

The investigation of the Hausdorff dimension for melonic D-balls requires a technical preamble. One denotes by S_q^n a certain sum of multinomial coefficients

$$S_q^n = \sum_{n_1,\dots n_q \geq 1}^{n_1+\cdots n_q = n} \frac{n!}{n_1! \dots n_q!}, \tag{7}$$

and sets $S_0^n = 0$. Remark at this point that $S_1^n = 1$ and $S_2^n = 2^n - 2$. In general, one has

Lemma 1.

$$S_q^n = \sum_{0 \leq r \leq q} (-1)^{q-r} \binom{q}{r} r^n. \tag{8}$$

Proof. See Appendix B. □

This technicality is of immediate use in something more practical below. To set up the following lemma, one should recall some points. Consider a vertex v in a melonic D-ball along with its word $w = (0; u_1 \dots u_n)$. One knows that the tree depth of v in the associated $(D+1)$-ary tree is simply $d_{\mathrm{T}}(v) = n$, while if $w = \tau_0 \tau_1 \dots \tau_k$, then the depth of v in the melonic D-ball is $d(v) = \Lambda(w) = k$.

Generically, there is not a simple formula relating $d_{\mathrm{T}}(v)$ and $d(v)$, that is, the tree depth with the depth. However, one can ask whether their average ratio $d(v)/d_{\mathrm{T}}(v) = \Lambda(w)/n$ approaches some value as $n \to \infty$. Said more precisely

Lemma 2. *Let $u_1, \dots, u_n$ be a sequence of random variables uniformly drawn from Σ_{D+1}, and denote $w = 0u_1 \dots u_n$. One has*

$$\frac{1}{n}\Lambda(w) \to_{n\to\infty} \Lambda_\Delta, \qquad \Lambda_\Delta^{-1} = (D+1)\sum_{0\le r\le D}(-1)^{D-r}\binom{D}{r}\frac{r}{(D+1-r)^2}. \tag{9}$$

Proof. Λ_Δ^{-1} is the average length of the τ_i for infinitely long w, that is, $\Lambda_\Delta^{-1} = \langle|\tau_i|\rangle$. Recalling the definition of the τ_i, one notes that $|\tau_0| = 1$ and $|\tau_1|$ is special: $|\tau_1| = (-1 +$ length of the sequence of letters that ends the first time the letter 0 appears). The probability P_n that this sequence ends after n letters is

$$\begin{aligned} P_1 &= \frac{1}{D+1}, \quad P_2 = (1-P_1)P_1, \quad P_3 = (1-P_1-P_2)P_1 = (1-P_1)^2P_1 \\ P_n &= (1-P_1-\cdots-P_{n-1}) \\ P_1 &= \big(1-P_1-(1-P_1)P_1-\cdots-(1-P_1)^{n-2}P_1\big)P_1 \\ &= (1-P_1)^{n-1}P_1. \end{aligned} \tag{10}$$

Hence

$$\begin{aligned} \langle|\tau_1|\rangle &= \sum_{n\ge1}(n-1)(1-P_1)^{n-1}P_1 = P_1\sum_{n\ge0}n(1-P_1)^n \\ &= P_1(1-P_1)(-\partial_{P_1})\frac{1}{1-(1-P_1)} \\ &= \frac{1-P_1}{P_1} = D < \infty. \end{aligned} \tag{11}$$

The finiteness of $\langle|\tau_1|\rangle$ implies that Λ_Δ^{-1} is the average length of τ_i, for $i \ge 2$.

One denotes by P_q^n the probability that after n draws one has obtained a sequence of letters with exactly q distinct colours. It follows that

$$\langle|\tau_i|\rangle = \sum_{n\ge1}(n-1)P_D^{n-1}\,P_1 = \frac{1}{D+1}\sum_{n\ge0}nP_D^n. \tag{12}$$

One needs a more explicit form of P_q^n. To this end, one notes that the probability of any fixed sequence of results on n draws is $\frac{1}{(D+1)^n}$. The number of configurations of n letters having n_1 times the colour i_1, n_2 times the colour i_2 up to n_q times the colour i_q is the multinomial coefficient:

$$\frac{n!}{n_1!\dots n_q!}. \tag{13}$$

As a result

$$P_q^n = \frac{1}{(D+1)^n}\binom{D+1}{q}\sum_{n_1,\dots n_q\geq 1}^{n_1+\dots n_q=n}\frac{n!}{n_1!\dots n_q!}$$
$$= \frac{1}{(D+1)^n}\binom{D+1}{q}\sum_{0\leq r\leq q}(-1)^{q-r}\binom{q}{r}r^n, \tag{14}$$

with the help of Lemma 1. There are two checks one needs to run on this formula. First, one checks that the probabilities are normalized:

$$\sum_{q=0}^{D+1}P_q^n = \frac{1}{(D+1)^n}\sum_{q=0}^{D+1}\binom{D+1}{q}\sum_{0\leq r\leq q}(-1)^{q-r}\binom{q}{r}r^n$$
$$= \frac{1}{(D+1)^n}\sum_{r=0}^{D+1}r^n\left[\sum_{q=r}^{D+1}\binom{D+1}{q}(-1)^{q-r}\binom{q}{r}\right] = 1, \tag{15}$$

by Eq. (85). Second, one checks that $P_q^n = 0$ for $n < q$:

$$\sum_{0\leq r\leq q}(-1)^{q-r}\binom{q}{r}r^n \sim [x\partial_x]^n(1-x)^q|_{x=1} = 0, \quad \text{for all } n < q. \tag{16}$$

One thus has

$$\langle|\tau_i|\rangle = \sum_{n\geq 0}nP_D^n\frac{1}{D+1} = \sum_{n\geq 0}n\frac{1}{(D+1)^n}\sum_{0\leq r\leq D}(-1)^{D-r}\binom{D}{r}r^n$$
$$= \sum_{0\leq r\leq D}(-1)^{D-r}\binom{D}{r}\sum_{n\geq 0}n\Big(\frac{r}{D+1}\Big)^n$$
$$= (D+1)\sum_{0\leq r\leq D}(-1)^{D-r}\binom{D}{r}\frac{r}{(D+1-r)^2}. \tag{17}$$

□

In particular for $D = 2, 3, 4$ one gets $\langle|\tau_i|\rangle = 9/2, 22/3, 125/12$, respectively.

Now let us make two remarks. First, Lemma 2 declares that, on average, the depth of a vertex in a melonic D-ball is, up to a constant rescaling by Λ_Δ, just the tree depth in the associated $(D+1)$-ary tree. Second, from the IID tensor model, one has that the Feynman weight of the melonic two-point graphs is equal to 1. Thus, the family of melonic D-balls corresponds to uniformly distributed trees. These two criteria set up an application of the non-trivial results established in [49], which leads one to the following conclusion:

Theorem 1. *Under the uniform distribution, the family of melonic D-balls converges in the Gromov–Hausdorff topology on compact metric spaces to the continuum random tree:*

$$\left(m_n, \frac{d_{m_n}}{\Lambda_\Delta \sqrt{\frac{(D+1)n}{D}}} \right) \longrightarrow_{n\to\infty} (\mathcal{T}_{2e}, d_{2e}). \tag{18}$$

While we relinquish most details to Appendix C, it might be beneficial to explain at least the concepts involved in the statement of Theorem 1.

One is familiar at this stage with the family of melonic D-balls. For the purposes of the theorem above, a melonic D-ball with n internal vertices is represented as a metric space: $(m_n, d_{m_n}/(\Lambda_\Delta \sqrt{(D+1)n/D}))$. Then, one looks at sequences of melonic D-balls, with increasing number of vertices, such that the element of the sequence at any given n is chosen randomly with respect to the uniform distribution at that n. The theorem states that, in the Gromov–Hausdorff topology on these associated metric spaces, the elements of such a sequence converge to the metric space known as the continuum random tree [54]: $(\mathcal{T}_{2e}, d_{2e})$.

A melonic *D*-ball as a metric space: One should have a certain familiarity at this stage with the family of melonic D-balls. With this in mind, one denotes a random melonic D-ball with n (internal) vertices by M_n. Then, one denotes this set of n vertices by m_n. As always, these n vertices are in correspondence with the n (elementary) vertices of the associated rooted coloured $(D+1)$-ary tree. Through this correspondence, there is a word associated with each element of m_n. As a result, one can put a lexicographical order on the elements m_n, that is, the vertices of m_n are ordered according to how their associated words occur in the dictionary. With respect to this order, one denotes the rth vertex in m_n by r for $r \in \{0, \ldots, n-1\}$ (and its associated word by $w(r)$). Then $d_{m_n}(r_1, r_2)$ is the graph distance between r_1 and r_2 in M_n. Just to be clear, $d_{m_n}(0, r)$ is the depth $\Lambda(w(r))$ defined earlier.

The distance between any two vertices can be well estimated from the depth. Consider two vertices r_1 and r_2 with words wu_0u and wv_0v. Thus, the two words have w in common, $u_0 \neq v_0$ are the first letters at which the two words differ and u and v denote the remaining letters in the words associated with r_1 and r_2. One denotes the vertices corresponding to w, wu_0 and wv_0 by r^s, r_1^s and r_2^s, respectively. One has $\Lambda(u_0u) = d_{m_n}(r_1^s, r_1)$ and $\Lambda(v_0v) = d_{m_n}(r_2^s, r_2)$.

The crucial point is that all the descendents of r_1^s (including r_1) are connected to the rest of the melonic ball by a path going necessarily through one of the vertices in the distance array of r_1^s (possibly r^s itself). One calls these vertices $r_1^{s;i}$, for $i \in \{0, \ldots D\}$. The same holds for r_2^s and r_2, and one denotes by $r_2^{s;j}, j \in \{0, \ldots D\}$ the vertices in the distance array of r_2^s. The distance between r_1^s and $r_1^{s;i}$ is at most 1. By the triangle inequality, in the triangle formed by r_1, r_1^s and $r_1^{s;i}$, one has

$$d_{m_n}(r_1, r_1^s) - 1 \leq d_{m_n}(r_1, r_1^{s;i}) \leq d_{m_n}(r_1, r_1^s) + 1 \qquad \forall i, \tag{19}$$

and similarly for the triangle formed by the three vertices r_2, r_2^s and $r_2^{s;j}$. The geodesic path from r_1 to r_2 passes through some fixed $r_1^{s;i}$ and $r_2^{s;j}$.

Hence, for some fixed i and j, one has

$$d_{m_n}(r_1, r_1^{s;i}) + d_{m_n}(r_2, r_2^{s;j}) \leq d_{m_n}(r_1, r_2). \tag{20}$$

On the other hand, the path $r_1 \to r_1^{s;i} \to r_1^s \to r^s \to r_2^s \to r_2^{s;j} \to r_2$ connects r_1 and r_2; hence

$$d_{m_n}(r_1, r_2) \leq d_{m_n}(r_1, r_1^{s;i}) + d_{m_n}(r_2, r_2^{s;j}) + 4, \tag{21}$$

and one concludes that

$$\begin{aligned} &d_{m_n}(r_1, r_1^s) + d_{m_n}(r_2, r_2^s) - 2 \leq d_{m_n}(r_1, r_2) \leq d_{m_n}(r_1, r_1^s) + d_{m_n}(r_2, r_2^s) + 6 \\ &\implies \left| d_{m_n}(r_1, r_2) - \Lambda(u_0 u) - \Lambda(v_0 v) \right| \leq 6. \end{aligned} \tag{22}$$

To make M_n a compact metric space, one needs a continuous metric. Thus, one must interpolate between the integer points on the integer grid (r_1, r_2), for $r_1, r_2 \in \{0, \ldots, n-1\}$. A piecewise linear interpolation on the triangles with integer co-ordinates $(r_1, r_2), (r_1+1, r_2), (r_1, r_2+1)$ and $(r_1+1, r_2+1), (r_1+1, r_2), (r_1, r_2+1)$ suffices.

As n gets large, one would like to ensure convergence to some compact metric space (rather than just letting the structure get infinitely large). This requires a n-dependent rescaling of metric. This is the genesis of the factor $\Lambda_\Delta \sqrt{(D+1)n/D}$. Then, $(m_n, d_{m_n}/(\Lambda_\Delta \sqrt{(D+1)n/D}))$ represents the melonic D-ball as a compact metric space.

A melonic *D*-ball as a random variable: It is worth noting that in the previous description M_n denotes a random melonic D-ball with n vertices. The set up of the (tensor) model ensures that at every n, the set of melonic D-balls is endowed with a uniform distribution. Thus, one draws a random melonic D-ball from this set according to this distribution. Moreover, this entails that in this context, convergence means stochastic convergence, that is, convergence in distribution.

Continuum Random Tree: A continuum random tree (CRT) $(\mathcal{T}_{2e}, d_{2e})$ is defined as a rooted real tree encoded by twice a normalized Brownian excursion e and endowed with a metric d_{2e}.

One is probably more familiar with rooted discrete trees, of which the coloured rooted $(D+1)$-ary trees are examples. Colored rooted $(D+1)$-ary trees (like all discrete trees) have an associated contour walk. Consider such a tree with n (elementary) vertices. (For simplicity, we shall consider its defoliated version, that is, all leaves removed.) Starting from the base of the tree, one traverses the perimeter of the tree, passing from one vertex to the next in unit time-steps. One considers the following continuous function $f(t)$, with $f(0) = 0$. As one travels, $f(i) = d_{\mathrm{T}}(v) + 1$, where v is the vertex one encounters at the ith time-step. (For the value at intermediate times, one linearly interpolates between the time-steps.) The procedure is illustrated in Fig. 9. Given the construction, one has that the journey ends at time-step $2n$, with $f(2n) = 0$ and $f(t) > 0$ for $0 < t < 2n$. One has thus associated with any tree some (fixed) walk f. For random trees with $2n$ vertices, the contour walk becomes a random walk with $2n$ steps.

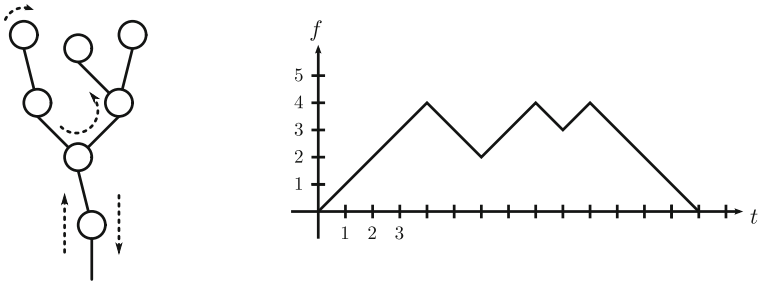

FIGURE 9. A defoliated $(D+1)$-ary tree and its associated contour walk

Any real continuous function $f(t)$, such that $f(0) = f(1) = 0$ and $f(t) > 0$ for $0 < t < 1$, encodes a rooted real tree $\mathcal{T}_f$. To get to the tree, one must set up the following equivalence: for all $s, t \in [0,1]$, set $m_f(s,t) = \inf_{\min(s,t) \le r \le \max(s,t)} f(r)$. Then

$$s \underset{f}{\sim} t \quad \Longleftrightarrow \quad f(s) = f(t) = m_f(s,t). \tag{23}$$

Then, the rooted real tree is the quotient: $\mathcal{T}_f = [0,1]/\underset{f}{\sim}$. The distance on the tree is given by

$$d_f(s,t) = f(s) + f(t) - 2m_f(s,t). \tag{24}$$

One can pick out the branching vertices of the tree as those values in $[0,1]$ that are congruent to two or more other values. This real tree differs from a discrete tree in that one has precise distance information along the edges of the tree.

The Wiener process is a stochastic process W_t (that is a random variable for every time t) such that $W_0 = 0, t \to W_t$ is almost surely continuous, W_t has independent increments and $W_t - W_s$ is distributed on a normal distribution of mean 0 and variance $\sigma^2 = t - s$ for $s \le t$. The normalized Brownian excursion e_t is a Wiener process conditioned to be positive for $0 < t < 1$ and be at 0 at time 1. It is formally represented by a the path integral measure

$$d\mu_e = \frac{1}{Z}\big[\mathrm{d}q(t)\big]\Big|_{\substack{q(0)=q(1)=0 \\ q(t)>0}} \mathrm{e}^{-\frac{1}{2}\int_0^1 [\dot{q}(t)]^2 \mathrm{d}t}, \tag{25}$$

with Z a normalization constant.

The CRT $(\mathcal{T}_{2e}, d_{2e})$ is the random tree associated with twice a normalized Brownian excursion $2e$.

Gromov–Hausdorff topology and convergence: Since one considers a sequence of random metric spaces, one should accurately define the space of metric spaces along with an appropriate topology. This is provided by the Gromov–Hausdorff topology on the space of isometry classes of compact metric spaces.

To begin, one considers a metric space (E, d_E). The Hausdorff distance between two compact sets, K_1 and K_2, in E is

$$d_{\mathrm{Haus}(E)}(K_1, K_2) = \inf\{r | K_1 \subset K_2^r, K_2 \subset K_1^r\}, \tag{26}$$

where $K_i^r = \bigcup_{x \in K_i} B_E(x, r)$ is the union of open balls of radius r centred on the points of K_i.

Now, given two compact metric spaces (E_i, d_i), the Gromov–Hausdorff distance between them is

$$d_{\mathrm{GH}}(E_1, E_2) = \inf\{d_{\mathrm{Haus}(E)}(\phi_1(E_1), \phi_2(E_2))\}, \tag{27}$$

where the infimum is taken on all metric spaces E and all isometric embeddings ϕ_1 and ϕ_2 from (E_1, d_1) and (E_2, d_2) into (E, d_E).

It emerges that $\mathbb{K}$, the set of all isometry classes of compact metric spaces, endowed with the Gromov–Hausdorff distance d_{GH} is a complete metric space in its own right. Therefore, one may study the convergence (in distribution) of $\mathbb{K}$-valued random variables.

Of course, the Gromov–Hausdorff topology is not the exclusive topology for these metric spaces, but fortuitously, it is well adapted to the study of quantities that are dependent on the size of the melonic D-balls, quantities such as the diameter, the depth, the distance between two random points and so forth.

Superficially, the Gromov–Hausdorff topology appears to be quite an eyeful. However, convergence in the Gromov–Hausdorff topology is a consequence of any convergence of (some sequence of) E_1 to E_2 embedded within a some common metric space E. In this case, the place of E_1 is taken by the sequence of random metric spaces M_n. Additionally, E_2 is the continuum random tree $\mathcal{T}_{2e}$ given in [54]. Then, the convergence claimed above rests on two points: (i) Skorohod's representation theorem states that there exists a metric space Ω, within which M_n (for all n) and $\mathcal{T}_{2e}$ can be embedded and is such that the image of d_{m_n} approaches the image of d_{2e} almost surely as $n \to \infty$; (ii) under the uniform distribution

$$\left(\frac{d_{m_n}(s_1 n, s_2 n)}{\Lambda_\Delta \sqrt{(D+1)n/D}}\right)_{(s_1,s_2)\in[0,1]^{\times 2}} \underset{n\to\infty}{\longrightarrow} \left(d_{2e}(s_1, s_2)\right)_{(s_1,s_2)\in[0,1]^{\times 2}}. \tag{28}$$

This second point is the result proven in the Appendix of [49] and to which we also devote Appendix C for explanation. It is clear that the involvement of Λ_Δ in the rescaling of the metric d_{m_n} is a highly subtle point.

Importantly, the Gromov–Hausdorff distance between M_n and $\mathcal{T}_{2e}$ is bounded from above by

$$\sup\left\{\left(d_{m_n}(s_1 n, s_2 n)/(\Lambda_\Delta \sqrt{(D+1)n/D}) - d_{2e}(s_1, s_2)\right) : (s_1, s_2) \in [0,1]^{\times 2}\right\}. \tag{29}$$

Thus, using Eq. (28), the stated convergence is ensured.

With the previous explanation, it is now clear that the Hausdorff dimension of the family of melonic D-balls may be read off from Eq. (18) as the inverse of the exponent of n in the rescaling of the metric. We formalise this in the following corollary:

Corollary 1. *The Hausdorff dimension of the family of melonic D-balls:*

$$d_{\mathrm{H}} = 2. \tag{30}$$

5. Spectral Dimension

One uncovers the spectral dimension of a structure by analysing an appropriate diffusion process on the structure in question. As a simple example, consider a diffusion process on a flat D-dimensional Euclidean geometry. One finds that the return probability attached to this process is $P(\sigma) \propto \sigma^{-D/2}$, where σ is the diffusion time. One may extract the spectral dimension by taking the logarithmic derivative

$$d_{\mathrm{S}} = -2\frac{d\log P(\sigma)}{d\log\sigma} = D. \tag{31}$$

Obviously, the spectral dimension coincides with the Hausdorff dimension in this elementary case, but this is not true in general.

In the case of the branched polymers phase arising in Dynamical Triangulations (where one deals with uncoloured binary trees), the appropriate diffusion process generates an average return probability, which in turn gives rise to a spectral dimension $d_{\mathrm{S}} = 4/3$. This was shown by Jonsson and Wheater in [48], using an argument that we shall follow rather closely.

It is worth mentioning, however, that for graphical structures, the spectral dimension depends rather strongly on the connectivity of the graph. This comes into play in the analysis below in that, a priori, one has a choice of graphical structure upon which one can place the diffusion process: the rooted melonic graphs, the melonic D-balls, the rooted coloured $(D+1)$-ary trees or even the stack D-spheres. We shall choose the rooted melonic graphs over and above the others. Although the direct analogue of the binary trees are the $(D+1)$-ary trees, the rooted melonic graphs are the topological dual to the melonic D-balls and so more directly capture the connectivity of the manifold. Meanwhile, a diffusion process on the melonic D-balls themselves is difficult to analyse. For rooted melonic graphs, the appropriate diffusion process generates a return/transit probability, where transit refers to the process of traversing from one external vertex to the other.[2] The spectral dimension is, however, still extracted from the return probability.

To proceed, consider a rooted melonic graph, with external colour 0, contributing to the connected 2-point function. Such a graph is drawn in Fig. 10.

[2] To be more precise, a diffusion process is characterized by the diffusion equation along with appropriate boundary conditions. For the rooted melonic graphs, it is appropriate to choose cyclic boundary conditions. This allows the interpretation of the process as occurring on a closed manifold, that is, the related closed melonic graphs.

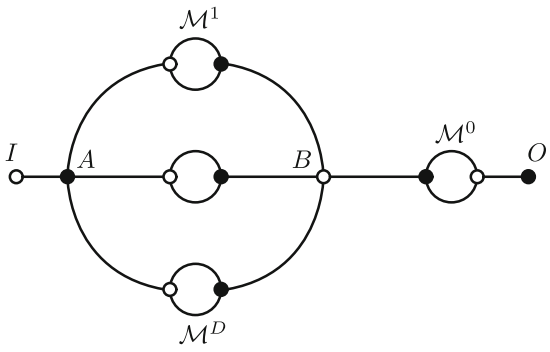

FIGURE 10. A rooted melonic graph $\mathcal{M}$ with sub-melons $\mathcal{M}^i$

One denotes it by $\mathcal{M}$. Due to its iterative structure, such a melon is constructed from $D+1$ rooted melonic graphs, each with a distinct external colour, connected in the fashion illustrated in Fig. 10. One denotes this property by $\mathcal{M} = \mathcal{M}^1 \cup \mathcal{M}^2 \cup \ldots \mathcal{M}^D \cup \mathcal{M}^0$, where $\mathcal{M}^i$ labelled the rooted melonic graph with external edges of colour i.

Any connected 2-point graph, hence any rooted melonic graph, has two external vertices, one white and one black. Unless distinguished by a special name, the white external vertex is referred to as $\circ$, while the black one is referred to as $\bullet$. For $\mathcal{M}$ itself, they are called, respectively, $\circ = I$ and $\bullet = O$.

First-return/first-transit probabilities: Consider a random walk on the melon $\mathcal{M}$. If the walker is at one of the external points, $\circ = I$ or $\bullet = O$, one can see from Fig. 10 that it steps with probability one to its unique neighbor. Meanwhile, if the walker is at any of the internal $(D+1)$-valent vertices, it steps with probability $\frac{1}{D+1}$ to one of its $D+1$ neighbors.

One denotes by $P^1_{\mathcal{M}}(t)$ the 2×2 matrix encoding the first-return/first-transit probabilities, in time t, for the rooted melonic graph $\mathcal{M}$. In detail, its four elements are

- $P^{1;\circ\circ}_{\mathcal{M}}(t) = P^{1;II}_{\mathcal{M}}(t)$, the probability that the walker starts from the external point $\circ = I$ and returns for the first time to $\circ = I$ at time t without touching the external point $\bullet = O$ in the intervening time.
- $P^{1;\circ\bullet}_{\mathcal{M}}(t) = P^{1;IO}_{\mathcal{M}}(t)$, the probability that the walker starts from the external point $\circ = I$ and reaches for the first time $\bullet = O$ at time t, without touching I a second time.
- $P^{1;\bullet\circ}_{\mathcal{M}}(t) = P^{1;OI}_{\mathcal{M}}(t)$, the probability that the walker starts from the external point $\bullet = O$ and reaches for the first time $\circ = I$ at time t without touching O a second time.
- $P^{1;\bullet\bullet}_{\mathcal{M}}(t) = P^{1;OO}_{\mathcal{M}}(t)$, the probability that the walker starts from the external point $\bullet = O$ and returns for the first time to $\bullet = O$ at time t without touching the external point $\circ = I$ in the intervening time.

Note that for any $\mathcal{M}, P^{1;\circ\circ}_{\mathcal{M}}(0) = P^{1;\circ\bullet}_{\mathcal{M}}(0) = P^{1;\bullet\circ}_{\mathcal{M}}(0) = P^{1;\bullet\bullet}_{\mathcal{M}}(0) = 0$. Moreover, the simplest melonic two point graph, denoted $\mathcal{M}_{(0)}$, consists of

exactly one line connecting the two external points. Its first-return/first-transit probability matrix is

$$P^1_{\mathcal{M}_{(0)}}(t) = \begin{pmatrix} 0 & \delta_{t,1} \\ \delta_{t,1} & 0 \end{pmatrix}. \tag{32}$$

Return/transit probability: Importantly, the first-return/first-transit probability matrix of $\mathcal{M}$ determines the return/transit probability matrix of $\mathcal{M}$ in time t, denoted by $P_{\mathcal{M}}(t)$. It is defined similarly to $P^1_{\mathcal{M}}(t)$, except that the walker is allowed any trajectory between the end and final points. Indeed, a generic path from $\circ = I$ to $\circ = I$ can be decomposed as a word on I and O starting and ending with I (for example, II, III, IOI and so on). Each pair of consecutive letters represent a walk from the first to the second letter that does not touch either external point in the intervening time. Similarly, a walk from $\circ = I$ to $\bullet = O$ can be decomposed as a word on I and O starting with I and ending with O. Let us denote by w_q, such words over I and O of length q, and denote $w_q(i)$ the ith letter of w_q. Then, the return/transit probability in time t is

$$\begin{aligned} P^{XY}_{\mathcal{M}}(t) &= \delta^{XY}\delta_{t,0} + P^{1;XY}_{\mathcal{M}}(t) + \sum_{q=1}^{\infty}\sum_{w_q}\sum_{t_0+\cdots+t_q=t} \\ &\times P^{1;Xw_q(1)}_{\mathcal{M}}(t_0) P^{1;w_q(1)w_q(2)}_{\mathcal{M}}(t_1)\ldots P^{1;w_q(q-1)w_q(q)}_{\mathcal{M}}(t_{q-1}) P^{1;w_q(q)Y}_{\mathcal{M}}(t_q). \end{aligned} \tag{33}$$

At this stage, one introduces generating functions for both quantities, $P^{1;XY}_{\mathcal{M}}(y) = \sum_t y^t P^{1;XY}_{\mathcal{M}}(t)$ and $P^{XY}_{\mathcal{M}}(y) = \sum_t y^t P^{XY}_{\mathcal{M}}(t)$. The above relation then becomes

$$\begin{aligned} P^{XY}_{\mathcal{M}}(y) &= \delta^{XY} + P^{1;XY}_{\mathcal{M}}(y) \\ &+ \sum_{q=1}^{\infty}\sum_{w_q} P^{1;Xw_q(1)}_{\mathcal{M}}(y) P^{1;w_q(1)w_q(2)}_{\mathcal{M}}(y)\ldots P^{1;w_q(q-1)w_q(q)}_{\mathcal{M}}(y) P^{1;w_q(q)Y}_{\mathcal{M}}(y). \end{aligned} \tag{34}$$

Noting that $w_q(1) \in \{I, O\}, w_q(2) \in \{I, O\}$ and so on, the above equation may be rewritten in matrix form (with obvious notation):

$$P_{\mathcal{M}}(y) = 1 + P^1_{\mathcal{M}}(y) + [P^1_{\mathcal{M}}(y)]^2 + \cdots = \frac{1}{1 - P^1_{\mathcal{M}}(y)}, \tag{35}$$

or in detail

$$\begin{aligned} \begin{pmatrix} P^{\circ\circ}_{\mathcal{M}}(y) & P^{\circ\bullet}_{\mathcal{M}}(y) \\ P^{\bullet\circ}_{\mathcal{M}}(y) & P^{\bullet\bullet}_{\mathcal{M}}(y) \end{pmatrix} &= \frac{1}{\left[1 - P^{1;\circ\circ}_{\mathcal{M}}(y)\right]\left[1 - P^{1;\bullet\bullet}_{\mathcal{M}}(y)\right] - P^{1;\bullet\circ}_{\mathcal{M}}(y) P^{1;\circ\bullet}_{\mathcal{M}}(y)} \\ &\times \begin{pmatrix} 1 - P^{1;\bullet\bullet}_{\mathcal{M}}(y) & P^{1;\circ\bullet}_{\mathcal{M}}(y) \\ P^{1;\bullet\circ}_{\mathcal{M}}(y) & 1 - P^{1;\circ\circ}_{\mathcal{M}}(y) \end{pmatrix}. \end{aligned} \tag{36}$$

Decomposition and iteration: The first-return/first-transit probability matrix of $\mathcal{M}$ can be computed in terms of the first-return/first-transit probability matrices of its sub-melons $\mathcal{M}^1, \dots, \mathcal{M}^D$ and $\mathcal{M}^0$.

A generic walk contributing to $(1, II)$ (that is, a walk starting at I and returning for the first time to I at time t, which does not touch O in the intervening time) can be further decomposed as a word over I, A, B, O (see Fig. 10). Starting with I, the walker first steps to A. Once at A, the possibilities increase. The walker may travel out from A and return without hitting B, or may traverse to B. Moreover, if the walker is at B at some time t, she may travel out (also in the direction of O, although never hit it) and return, or may traverse back to A. These sub-paths may occur any number of times before eventually the walker returns to A a last time and steps back to I. Similarly, a walk contributing to $(1, IO)$ starts from I, passes through A, then A and B a number of times, before finally going to B a last time and jumping to O. Thus

$$\begin{aligned}(1, II) &= I\ A \dots AB \dots BA \dots A\ I\\ (1, IO) &= I\ A \dots AB \dots BA \dots AB \dots B\ O\\ (1, OI) &= O\ B \dots BA \dots A\ I\\ (1, OO) &= OO \text{ or } O\ B \dots BA \dots AB \dots B\ O\end{aligned} \tag{37}$$

While $(1, OI)$ is described similarly to $(1, IO)$, the are more walks than one might expect contributing to $(1, OO)$. Indeed, there are walks, signified above by OO, that start from O, go into the melon $\mathcal{M}^0$ and return to O without ever touching B.

The first-return/first-transit probabilities between A and B may be written in terms of the first-return/ first-transit probabilities for the sub-melons: $\mathcal{M}^1, \dots, \mathcal{M}^D$ and $\mathcal{M}^0$. Indeed, for a random walk to go from say A to A it needs to chose one of the sub-melons $\mathcal{M}^1, \dots \mathcal{M}^D$ and go from $\bullet$ to $\bullet$ in it. Thus

$$\begin{aligned}P^{1;AA}(t) &= \frac{1}{D+1}\Big(P^{1,\bullet\bullet}_{\mathcal{M}^1}(t) + \dots + P^{1,\bullet\bullet}_{\mathcal{M}^D}(t)\Big)\\ P^{1;AB}(t) &= \frac{1}{D+1}\Big(P^{1,\bullet\circ}_{\mathcal{M}^1}(t) + \dots + P^{1,\bullet\circ}_{\mathcal{M}^D}(t)\Big)\\ P^{1;BA}(t) &= \frac{1}{D+1}\Big(P^{1,\circ\bullet}_{\mathcal{M}^1}(t) + \dots + P^{1,\circ\bullet}_{\mathcal{M}^D}(t)\Big)\\ P^{1;BB}(t) &= \frac{1}{D+1}\Big(P^{1,\circ\circ}_{\mathcal{M}^1}(t) + \dots + P^{1,\circ\circ}_{\mathcal{M}^D}(t) + P^{1,\circ\circ}_{\mathcal{M}^0}(t)\Big),\end{aligned} \tag{38}$$

where again one notes that the first return probability for B to B is special, as the walk may go also into the melon $\mathcal{M}^0$. (Note that on the right hand side of Eq. (38), $\bullet = A$ and $\circ = B$.) Denoting by $P^1(t)$ the first-return/first-transit probability matrix between A and B, one has

$$P^1(t) = \frac{1}{D+1}P^1_{\mathcal{M}^1}(t) + \dots + \frac{1}{D+1}P^1_{\mathcal{M}^D}(t) + \frac{1}{D+1}\begin{pmatrix} P^{1,\circ\circ}_{\mathcal{M}^0}(t) & 0\\ 0 & 0\end{pmatrix}. \tag{39}$$

Furthermore, the first-return/first-transit probabilities between B and O are

$$P^{1;OB}(t) = P^{1,\bullet\circ}_{\mathcal{M}^0}(t), \quad P^{1;BO}(t) = \frac{1}{D+1} P^{1,\circ\bullet}_{\mathcal{M}^0}(t), \quad P^{1;OO}(t) = P^{1,\bullet\bullet}_{\mathcal{M}^0}(t). \tag{40}$$

On this occasion, let us denote by w_q the words of q letters over A and B. The walks of first-return starting and ending with I decompose as

$$\begin{aligned} P^{1,\circ\circ}_{\mathcal{M}}(t) &= \frac{1}{D+1}\delta_{t,2} + \frac{1}{D+1} P^{1;AA}(t-2) \\ &< + \frac{1}{D+1} \sum_{q=1}^{\infty} \sum_{w_q} \sum_{t_0+\cdots+t_q=t-2} \\ &\quad \Big(P^{1;Aw_q(1)}(t_0) P^{1;w_q(1)w_q(2)}(t_1) \dots P^{1;w_q(q-1)w_q(q)}(t_{q-1}) P^{1;w_q(q)A}(t_q) \Big). \end{aligned} \tag{41}$$

The first step of the walk is from I to A. At the second step, the walker either returns with probability $(D+1)^{-1}$ to I (the first term) or proceeds down one of the sub-melons $\mathcal{M}^1, \dots, \mathcal{M}^D$. The walker can then either return to A without touching B in $t-2$ steps and go to I with probability $(D+1)^{-1}$ at the last step (the second term), or go from A to B a number of times, end in A and jump with probability $(D+1)^{-1}$ at the last step in I (all the other terms). Similar considerations lead to the following equations:

$$\begin{aligned} P^{1,\circ\bullet}_{\mathcal{M}}(t) &= \sum_{t_0+t_1=t-1} P^{1;AB}(t_0) P^{1;BO}(t_1) \\ &+ \sum_{q=1}^{\infty} \sum_{w_q} \sum_{t_0+\cdots+t_{q+1}=t-1} \Big(P^{1;Aw_q(1)}(t_0) \dots P^{1;w_q(q)B}(t_q) P^{1;BO}(t_{q+1}) \Big), \\ P^{1,\bullet\circ}_{\mathcal{M}}(t) &= \frac{1}{D+1} \sum_{t_0+t_1=t-1} P^{1;OB}(t_0) P^{1;BA}(t_1) \\ &+ \frac{1}{D+1} \sum_{q=1}^{\infty} \sum_{w_q} \sum_{t_0+\cdots+t_{q+1}=t-1} \Big(P^{1;OB}(t_0) P^{1;Bw_q(1)}(t_1) \dots P^{1;w_q(q)A}(t_{q+1}) \Big), \\ P^{1,\bullet\bullet}_{\mathcal{M}}(t) &= P^{1;OO}(t) + \sum_{t_0+t_1=t} P^{1;OB}(t_0) P^{1;BO}(t_1) \\ &+ \sum_{t_0+t_1+t_2=t} P^{1;OB}(t_0) P^{1;BB}(t_1) P^{1;BO}(t_2) \\ &+ \sum_{q=1}^{\infty} \sum_{w_q} \sum_{t_0+\cdots+t_{q+2}=t} \\ &\quad \Big(P^{1;OB}(t_0) P^{1;Bw_q(1)}(t_1) \dots P^{1;w_q(q)B}(t_{q+1}) P^{1;BO}(t_{q+2}) \Big). \end{aligned} \tag{42}$$

As one might expect, $P^{1;OO}_{\mathcal{M}}(t)$ requires special consideration. The first term, $P^{1;OO}(t)$, represents the walks which start from O and end in O without touching B. As before, the equations simplify for generating functions:

$$\begin{aligned}
P^{1,\circ\circ}_{\mathcal{M}}(y) &= \frac{1}{D+1}y^2 + \frac{1}{D+1}y^2 P^{1;AA}(y) \\
&\quad + \frac{1}{D+1}y^2 \sum_{q=1}^{\infty} P^{1;Aw_q(1)}(y) P^{1;w_q(1)w_q(2)}(y) \dots P^{1;w_q(q)A}(y) \\
P^{1,\circ\bullet}_{\mathcal{M}}(y) &= yP^{1;AB}(y)P^{1;BO} \\
&\quad + y \sum_{q=1}^{\infty} P^{1;Aw_q(1)}(y) P^{1;w_q(1)w_q(2)}(y) \dots P^{1;w_q(q)B}(y) P^{1;BO}(y) \\
P^{1,\bullet\circ}_{\mathcal{M}}(y) &= \frac{1}{D+1}yP^{1;OB}(y)P^{1;BA}(y) \\
&\quad + \frac{1}{D+1}y \sum_{q=1}^{\infty} P^{1;OB}(y) P^{1;Bw_q(1)}(y) P^{1;w_q(1)w_q(2)}(y) \dots P^{1;w_q(q)A}(y) \\
P^{1,\bullet\bullet}_{\mathcal{M}}(y) &= P^{1;OO}(y) + P^{1;OB}(y)P^{1;BO}(y) + P^{1;OB(y)}P^{1;BB}(y)P^{1;BO}(y) \\
&\quad + \sum_{q=1}^{\infty} P^{1;OB}(y) P^{1;Bw_q(1)}(y) P^{1;w_q(1)w_q(2)}(y) \dots P^{1;w_q(q)B}(y) P^{1;BO}(y).
\end{aligned} \tag{43}$$

Furthermore, in matrix form, they look yet simpler:

$$\begin{aligned}
P^{1}_{\mathcal{M}}(y) &= \begin{pmatrix} 0 & 0 \\ 0 & P^{1;OO}(y) \end{pmatrix} \\
&\quad + \begin{pmatrix} y & 0 \\ 0 & P^{1;OB}(y) \end{pmatrix} \sigma \Big[1 - P^{1}(y)\Big]^{-1} \sigma \begin{pmatrix} \frac{y}{D+1} & 0 \\ 0 & P^{1;BO}(y) \end{pmatrix},
\end{aligned} \tag{44}$$

where

$$\sigma = \begin{pmatrix} 0 & 1 \\ 1 & 0 \end{pmatrix}. \tag{45}$$

Substituting the various probabilities as a function of the sub-melons one gets a recursive equation along with an initial condition:

$$\begin{aligned}
P^{1}_{\mathcal{M}}(y) &= \begin{pmatrix} 0 & 0 \\ 0 & P^{1,\bullet\bullet}_{\mathcal{M}^0}(y) \end{pmatrix} + \frac{1}{D+1} \begin{pmatrix} y & 0 \\ 0 & P^{1,\bullet\circ}_{\mathcal{M}^0}(y) \end{pmatrix} \\
&\quad \times \sigma \left[1 - \frac{1}{D+1} \left(P^{1}_{\mathcal{M}^1}(y) + \dots P^{1}_{\mathcal{M}^D}(y) + \begin{pmatrix} P^{1,\circ\circ}_{\mathcal{M}^0}(t) & 0 \\ 0 & 0 \end{pmatrix} \right) \right]^{-1} \\
&\quad \times \sigma \begin{pmatrix} y & 0 \\ 0 & P^{1,\circ\bullet}_{\mathcal{M}^0}(y) \end{pmatrix},
\end{aligned} \tag{46}$$

$$P^{1}_{\mathcal{M}_{(0)}}(y) = \begin{pmatrix} 0 & y \\ y & 0 \end{pmatrix}.$$

In principle, this solves the problem of determining the first-return/first-transit probabilities for an arbitrary melon. For example, the first non-trivial melon

is the elementary melon of colour 0, denoted by $\mathcal{M}_{(1)}$, and one gets

$$P^1_{\mathcal{M}_{(1)}}(y) = \frac{1}{D+1}\begin{pmatrix} y & 0 \\ 0 & y \end{pmatrix}\left[1 - \frac{D}{D+1}\begin{pmatrix} 0 & y \\ y & 0 \end{pmatrix}\right]^{-1}\begin{pmatrix} y & 0 \\ 0 & y \end{pmatrix}$$
$$= \frac{\frac{1}{D+1}y^2}{1-\frac{D^2}{(D+1)^2}y^2}\begin{pmatrix} 1 & \frac{D}{D+1}y \\ \frac{D}{D+1}y & 1 \end{pmatrix}. \tag{47}$$

Defining some auxiliary 2×2 matrices cleans up the formulae quite significantly:

$$E^{ab}_{\alpha\beta} = \delta^a_\alpha\,\delta^b_\beta \qquad \text{where} \qquad a,b,\alpha,\beta \in \{1,2\}. \tag{48}$$

Thus

$$P^1_{\mathcal{M}} = E^{22}P^1_{\mathcal{M}^0}E^{22} + \left(E^{12}y + E^{22}P^1_{\mathcal{M}^0}E^{11}\right)$$
$$\times\frac{1}{D+1-\sum_{i=1}^D P^1_{\mathcal{M}^i} - E^{11}P^1_{\mathcal{M}^0}E^{11}}\left(yE^{21} + E^{11}P^1_{\mathcal{M}^0}E^{22}\right) \tag{49}$$
$$P^1_{\mathcal{M}_{(0)}} = \begin{pmatrix} 0 & y \\ y & 0 \end{pmatrix} \equiv y\,\sigma.$$

Note that by induction one trivially obtains that the first-return/first-transit matrix is symmetric

$$P^{1,\bullet\circ}_{\mathcal{M}}(y) = P^{1,\circ\bullet}_{\mathcal{M}}(y). \tag{50}$$

Ultimately, one must solve this system to obtain a closed form for the return/transit probability and thereafter extract the spectral dimension. Suggestively, the matrix form of the system in Eq. (47) has superficial similarities to the system given in [48]. However, in comparison with [48], there are two added complications: (i) it is a matrix rather than a scalar equation; (ii) the final term in the denominator obscures a direct recursive solution. To circumvent these problems, one considers first so-called simple melons. Later, we shall argue that the general case is just a small correction that does not affect the spectral dimension.

Simple Melons: Simple melons are those rooted melonic graphs $\mathcal{M}$ conditioned by (i) $\mathcal{M}^0 = \emptyset$ and (ii) for $\mathcal{N}$ any sub-melon of colour i in $\mathcal{M}$, then $\mathcal{N}^i = \emptyset$. In terms of the associated $(D+1)$-ary tree, a simple melon corresponds to a tree such that no branch possesses two consecutive lines of the same colour. Then, the final term in the denominator vanishes and the formula reduces to

$$P^1_{\mathcal{M}} = y^2\sigma\frac{1}{D+1-\sum_{i=1}^D P^1_{\mathcal{M}^i}}\sigma \tag{51}$$

Lemma 3. *$P^1_{\mathcal{M}} = a + b\sigma$ for all simple melons $\mathcal{M}$, where $a,b \in \mathbb{R}$ and a implicitly multiplies the 2×2 identity matrix.*

Proof. First of all, $P^1_{\mathcal{M}_{(0)}} = y\sigma$, so it is of the claimed form. Then, one uses an inductive argument. One notices the following general matrix relationship:

$$\sigma(\alpha+\beta\sigma)^{-1}\sigma = \sigma\left(\frac{\alpha}{\alpha^2-\beta^2} - \frac{\beta}{\alpha^2-\beta^2}\sigma\right)\sigma = \frac{\alpha}{\alpha^2-\beta^2} - \frac{\beta}{\alpha^2-\beta^2}\sigma. \tag{52}$$

Thus, should each $P^1_{\mathcal{M}^i}$ be of the claimed form, one can use Eq. (52) to rewrite $P^1_{\mathcal{M}}$ in the same form. □

Noting moreover that $\sigma(a+b\sigma)\sigma = a+b\sigma$, it follows that the recursion may be rewritten as

$$P^1_{\mathcal{M}} = y^2 \frac{1}{D+1-\sum_{i=1}^D P^1_{\mathcal{M}^i}}, \tag{53}$$

and that all the $P^1_{\mathcal{M}^i} = a_i + b_i\sigma$ may be diagonalized simultaneously on the following basis: $\frac{1}{\sqrt{2}}\begin{pmatrix}1\\1\end{pmatrix}, \frac{1}{\sqrt{2}}\begin{pmatrix}1\\-1\end{pmatrix}$, with eigenvalues $\lambda^1_{\mathcal{M}^i;(1,2)} = a_i \pm b_i$, that is,

$$P^1_{\mathcal{M}} = \frac{1}{2}\begin{pmatrix}1 & 1\\1 & -1\end{pmatrix}\begin{pmatrix}\lambda^1_{\mathcal{M};1} & 0\\0 & \lambda^1_{\mathcal{M};2}\end{pmatrix}\begin{pmatrix}1 & 1\\1 & -1\end{pmatrix}. \tag{54}$$

In its diagonalized form, the recursion is

$$\begin{pmatrix}\lambda^1_{\mathcal{M};1} & 0\\0 & \lambda^1_{\mathcal{M};2}\end{pmatrix} = \begin{pmatrix}\frac{y^2}{D+1-\sum_i \lambda^1_{\mathcal{M}^i;1}} & 0\\0 & \frac{y^2}{D+1-\sum_i \lambda^1_{\mathcal{M}^i;2}}\end{pmatrix},$$
$$\lambda^1_{\mathcal{M}_{(0)};1} = y, \quad \lambda^1_{\mathcal{M}_{(0)};2} = -y. \tag{55}$$

Thus, one may restate the scalar recursion for each eigenvalue in terms of a single $\lambda_{\mathcal{M}}(y)$:

$$\lambda_{\mathcal{M}}(y) = \frac{y^2}{D+1-\sum_i \lambda_{\mathcal{M}^i}(y)} \quad \text{and} \quad \lambda_{\mathcal{M}_{(0)}}(y) = y, \tag{56}$$

with $\lambda^1_{\mathcal{M};1} = \lambda_{\mathcal{M}}(y)$ and $\lambda^1_{\mathcal{M};2} = \lambda_{\mathcal{M}}(-y)$. At this stage, the system for $\lambda_{\mathcal{M}}(y)$ has almost coincided with that of [48]. However, one must still tread carefully: first the powers of y differ with respect to [48] and second, one must deal with the extension to $D+1$ colours. The argument is checked below. First, one introduces the function

$$h_{\mathcal{M}}(y) = \frac{1}{1-y}(1-\lambda_{\mathcal{M}}(y)), \tag{57}$$

so that the recursion may be rewritten once again as

$$h_{\mathcal{M}}(y) = \frac{1+y+\sum_i h_{\mathcal{M}^i}(y)}{1+(1-y)\sum_i h_{\mathcal{M}^i}(y)} \quad \text{and} \quad h_{\mathcal{M}_{(0)}}(y) = \frac{1}{1-y}(1-y) = 1. \tag{58}$$

One defines the generating function:

$$Q(z,y) = \sum_{\mathcal{M}} z^p \frac{1}{1-\lambda_{\mathcal{M}}(y)} = \sum_{\mathcal{M}} z^p \frac{1}{(1-y)}\frac{1}{h_{\mathcal{M}}(y)}, \tag{59}$$

One can show that $Q(z,y)$ has a simple pole at $y=1$ by showing that the sum $\sum_{\mathcal{M}} z^p/h_{\mathcal{M}}(1)$ converges. At $y=1$, the recursion and initial condition are given by

$$h_{\mathcal{M}}(1) = 2 + \sum_i h_{\mathcal{M}^i}(1) \quad \text{and} \quad h_{\mathcal{M}_{(0)}}(1) = 1. \tag{60}$$

If the melon $\mathcal{M}$ has $2p$ internal vertices, the contribution of the pole to the sum is

$$h_{\mathcal{M}}(1) = 2 + \sum_i [(D+1)p_i + 1] = 2 + D + (D+1)\sum_i p_i = (D+1)p + 1, \quad (61)$$

where one takes into account that the melon $\mathcal{M}$ with $2p$ vertices satisfies $p = \sum_i p_i + 1$, if the sub-melons $\mathcal{M}^i$ have $2p_i$ vertices. Thus,

$$(1-y)Q(z,y)\big|_{y=1} = \sum_{p\geq 0} z^p C_p \frac{1}{(D+1)p+1},$$
$$\text{where} \quad C_p = \frac{1}{Dp+1}\binom{Dp+1}{p}, \quad (62)$$

which converges for $z < \frac{(D-1)^{D-1}}{D^D} = z_0$.

The information about the spectral dimension is contained the remaining non-pole part, so one defines

$$\widetilde{Q}(z,y) = -\frac{\mathrm{d}}{\mathrm{d}y}(1-y)Q(z,y) = \sum_{\mathcal{M}} z^p \frac{1}{h_{\mathcal{M}}(y)^2}\frac{\mathrm{d}}{\mathrm{d}y}h_{\mathcal{M}}(y). \quad (63)$$

Rather than tackle $\widetilde{Q}(z,y)$ all in one go, one concentrates for a moment on $\widetilde{Q}_n(z)$, where

$$\widetilde{Q}(z,y) = \sum_{n\geq 0}\frac{(y-1)^n}{n!}\widetilde{Q}_n(z), \quad (64)$$

so that

$$\widetilde{Q}_n(z) = \frac{\mathrm{d}^n}{\mathrm{d}y^n}\widetilde{Q}(z,y)|_{y=1} = -\sum_{\mathcal{M}} z^p \frac{\mathrm{d}^{n+1}}{\mathrm{d}y^{n+1}}\frac{1}{h_{\mathcal{M}}(y)}\Big|_{y=1}. \quad (65)$$

Defining further

$$h_{\mathcal{M}}^{(n)} = \frac{\mathrm{d}^n}{\mathrm{d}y^n}h_{\mathcal{M}}(y)\Big|_{y=1}, \quad (66)$$

one can express

$$\widetilde{Q}_n(z) = \sum_{r=1}^{n+1}(-1)^{r+1}\, r! \sum_{\substack{a_1,\ldots,a_{n+1} \\ \sum a_j = r\,;\, \sum j a_j = n+1}} \frac{(n+1)!}{(1!)^{a_1}\ldots[(n+1)!]^{a_{n+1}}a_1!\ldots a_{n+1}!}$$
$$\sum_{\mathcal{M}} z^p \frac{\prod_j \left[h_{\mathcal{M}}^{(j)}\right]^{a_j}}{\left[h_{\mathcal{M}}^{(0)}\right]^{r+1}}, \quad (67)$$

where more details are given in Eqs. (47)–(52) of [48]. From this point on, we change notation slightly. We shall use $N_{\mathcal{M}}$ to denote half the number of vertices in $\mathcal{M}$, while p will represent the number of indices in subsequent formulae (we do this to keep notational similarity to the analogous argument given in Sect. 5 of [48]).

We denote

$$H^{(n_1,\ldots n_p)}(z) := \sum_{\mathcal{M}} z^{N_{\mathcal{M}}}\, h_{\mathcal{M}}^{(n_1)} h_{\mathcal{M}}^{(n_2)} \ldots h_{\mathcal{M}}^{(n_p)}. \quad (68)$$

In order to derive the asymptotic behaviour of $\widetilde{Q}_n(z)$ we first note that

$$\begin{aligned}
&\Big((D+1)z\frac{\partial}{\partial z}+1\Big)^{r+1}\left(\sum_{\mathcal{M}} z^{N_{\mathcal{M}}}\ \frac{\prod_j \big(h^{(j)}_{\mathcal{M}}\big)^{a_j}}{\big(h^{(0)}_{\mathcal{M}}\big)^{r+1}}\right)\\
&\quad=\sum_{\mathcal{M}} z^{N_{\mathcal{M}}}\Big[(D+1)N_{\mathcal{M}}+1\Big]^{r+1}\frac{\prod_j \big(h^{(j)}_{\mathcal{M}}\big)^{a_j}}{\big(h^{(0)}_{\mathcal{M}}\big)^{r+1}}\\
&\quad=\sum_{\mathcal{M}} z^{N_{\mathcal{M}}}\prod_j \big(h^{(j)}_{\mathcal{M}}\big)^{a_j}=H^{(a_1\otimes 1,\dots,a_{n+1}\otimes n+1)}\,,\qquad a_i\otimes i\equiv\underbrace{i,\dots i}_{a_i},
\end{aligned}\tag{69}$$

where we used Eqs. (61) and (66). Thus the asymptotic behaviour of the term of order r in Eq. (67) can be obtained by integrating $r+1$ times the asymptotic behaviour of $H^{(a_1\otimes 1,\dots,a_{n+1}\otimes n+1)}$. We show in Appendix D that

Lemma 4. *For all $n_1,\dots n_p$ the following asymptotic behaviour holds:*

$$\begin{aligned}
H^{(n_1,\dots n_p)}(z):=\sum_{\mathcal{M}} z^{N_{\mathcal{M}}}\ h^{(n_1)}_{\mathcal{M}}h^{(n_2)}_{\mathcal{M}}\dots h^{(n_p)}_{\mathcal{M}}\sim u^{\frac{1}{2}-p-\frac{3}{2}(n_1+n_2+\dots+n_p)},\\
\text{as}\quad z\uparrow z_0,
\end{aligned}\tag{70}$$

with $u=1-z/z_0$. In particular

$$H^{(a_1\otimes 1,\dots,a_{n+1}\otimes n+1)}\sim u^{\frac{1}{2}-r-\frac{3}{2}(n+1)}.\tag{71}$$

Substituting the leading order behaviour Eq. (71) and integrating $r+1$ times, one obtains the leading order behaviour:

$$\widetilde{Q}_0(z)\sim\log(1-z/z_0),\qquad \widetilde{Q}_n(z)\sim(1-z/z_0)^{-\frac{3}{2}n},\quad \forall n>0.\tag{72}$$

Consequently, the most singular part of $\widetilde{Q}(z,y)$ as $z\uparrow z_0$ is the sum of logarithmic piece and a function of $(1-y)(1-z/z_0)^{-\frac{3}{2}}$. Thus, one arrives at an expression which is identical to Eq. (57) in [48]:

$$\frac{\partial\widetilde{Q}}{\partial z}(z,y)=\frac{1}{1-z/z_0}\ \ \widetilde{\Phi}\left(\frac{1-y}{(1-z/z_0)^{\frac{3}{2}}}\right),\tag{73}$$

for some function $\widetilde{\Phi}$. The rest of the analysis coincides exactly with the one given in [48, Sect. 4.2] so that the spectral dimension of the family of simple melons is $d_{\mathrm{S}}=4/3$.

There are two comments to make here. The first point to note is that the $\partial\widetilde{Q}/\partial z$ obtained in Eq. (73) pertains to the system for $\lambda_{\mathcal{M}}(y)$ with initial condition $\lambda_{\mathcal{M}_{(0)}}(y)=y$, that is, to $\lambda^1_{\mathcal{M};1}(y)$. One should recall that this scalar problem arose via the diagonalization of a matrix problem. So, a priori, it does not simply provide the behaviour of the return probability, but rather the sum of this and the return/transit probability. To remedy this, one should repeat the process for the system with initial condition $\lambda_{\mathcal{M}_{(0)}}(y)=-y$. The resulting $Q(z,y)$ has a pole at $y=-1$ and after removing this, one finds that the same procedure leads to Eq. (73), except with $y\to -y$ on the right-hand side. This provides the behaviour of the difference of the return probability and the

return/transit probability. By following an argument analogous to that given in Sect. 4.2 of [48], for the quantity

$$\begin{aligned}&\frac{\partial\widetilde{Q}}{\partial z}(z,y)+\frac{\partial\widetilde{Q}}{\partial z}(z,-y)\\&\quad=\frac{1}{1-z/z_0}\ \widetilde{\Phi}\left(\frac{1-y}{(1-z/z_0)^{\frac{3}{2}}}\right)+\frac{1}{1-z/z_0}\ \widetilde{\Phi}\left(\frac{1+y}{(1-z/z_0)^{\frac{3}{2}}}\right),\end{aligned}\tag{74}$$

in the regime $|y|<1$, one extracts the behaviour of the return probability, and the spectral dimension stated in Eq. (75).

The second comment refers to the non-simple melons, which have been neglected up to this point. We argue rather indirectly that their inclusion has a negligible effect on the spectral dimension. Durhuus et al. have shown in [56] that the spectral dimension of the infinite Galton–Watson tree is 4/3. We explain in Appendix C that rooted melonic graphs correspond to such objects in the infinite limit. To establish $d_{\mathrm{S}}=4/3$ using this line of reasoning, one would have to have to repeat that analysis again with colour information and so forth. Although we do not do this in detail, the results we provide here overwhelmingly back up this claim. Therefore, we are in a position to state

Theorem 2. *The spectral dimension of the family of melonic graphs*

$$d_{\mathrm{S}}=\frac{4}{3}.\tag{75}$$

Acknowledgements

We thank Vincent Rivasseau for discussions.

Appendix A. The Road to Melonic Graphs

Let us construct the class of independent identically distributed (IID) models. We shall attempt to be precise without being especially detailed. We refer the reader to [57] for a more thorough explanation. The fundamental variable is a complex rank-D tensor, which may be viewed as a map $T:H_1\times\cdots\times H_D\to\mathbb{C}$, where the H_i are complex vector spaces of dimension N_i. It is a tensor, so it transforms covariantly under a change of basis of each vector space independently. Its complex-conjugate $\overline{T}$ is its contravariant counterpart.

One refers to their components in a given basis by T_n and $\overline{T}_{\bar{n}}$, where $n=\{n_1,\ldots,n_D\},\bar{n}=\{\bar{n}_1,\ldots,\bar{n}_D\}$ and the bar $(-)$ distinguishes contravariant from covariant indices.

As one might imagine, with these two ingredients, one can build objects that are invariant under changes of bases. These so-called trace invariants are a subset of $(T,\overline{T})$-dependent monomials that are built by pairwise contracting covariant and contravariant indices until all indices are saturated. It emerges readily that the pattern of contractions for a given trace invariant is associated

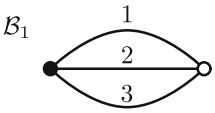

$$\mathrm{tr}_{\mathcal{B}_1}(T,\overline{T}) = T_{n_1 n_2 n_3}\,\delta_{n_1\bar{n}_1}\,\delta_{n_2\bar{n}_2}\,\delta_{n_3\bar{n}_3}\,\overline{T}_{\bar{n}_1\bar{n}_2\bar{n}_3}$$

FIGURE 11. A closed D-colored graph and its associated trace invariant (for $D = 3$)

with a unique closed D-coloured graph, in the sense that given such a graph, one can reconstruct the corresponding trace invariant and vice versa.[3]

In Fig. 11, we illustrate the graph $\mathcal{B}_1$, the unique closed D-coloured graph with two vertices, which represents the unique quadratic trace invariant $\mathrm{tr}_{\mathcal{B}_1}(T,\bar{T}) = T_n\,\delta_{n\bar{n}}\,\overline{T}_{\bar{n}}$.

More generally, we denote the trace invariant corresponding to the graph $\mathcal{B}$ by $\mathrm{tr}_{\mathcal{B}}(T,\bar{T})$.

From now on, we shall make two restrictions: (i) all the vector spaces have the same dimension N and (ii) we consider only connected trace invariants, that is, trace invariants corresponding to graphs with just a single connected component.

Given these provisos, the most general invariant action for such tensors is

$$S(T,\bar{T}) = \mathrm{tr}_{\mathcal{B}_1}(T,\bar{T}) + \sum_{k=2}^{\infty}\sum_{\mathcal{B}\in\Gamma_k^{(D)}} \frac{t_{\mathcal{B}}}{N^{\frac{2}{(D-2)!}\omega(\mathcal{B})}}\,\mathrm{tr}_{\mathcal{B}}(T,\bar{T}), \tag{76}$$

where $\Gamma_k^{(D)}$ is the set of connected closed D-coloured graphs with $2k$ vertices, $\{t_{\mathcal{B}}\}$ is the set of coupling constants and $\omega(\mathcal{B}) \geq 0$ is the degree of $\mathcal{B}$ (see [1] for its definition and properties). This defines the IID class of models.

A.1. Free Energy and Melonic Graphs

The central objects for further investigation emerge from the free energy (per degree of freedom) associated with these models:

$$E(\{t_{\mathcal{B}}\}) = -\frac{1}{N^D}\log\left(\int \mathrm{d}T\,\mathrm{d}\bar{T}\;\mathrm{e}^{-N^{D-1}S(T,\bar{T})}\right). \tag{77}$$

[3] While we refer the reader to [1] for various definitions, it is perhaps not unwise to match up right here the defining properties of a closed D-coloured graph $\mathcal{B}$ with those of a trace invariant:

- $\mathcal{B}$ has two types of vertex, labelled black and white, that represent the two types of tensor, T and $\bar{T}$, respectively.
- Both types of vertex are D-valent, with matches the property that both types of tensor have D indices.
- $\mathcal{B}$ is bipartite, meaning that black vertices are directly joined only to white vertices and vice versa. This is in correspondence with the fact that indices are contracted in covariant–contravariant pairs.
- Every edge of $\mathcal{B}$ is coloured by a single element of $\{1,\ldots,D\}$, such that the D edges emanating from any given vertex possess distinct colours. This represents the fact that the indices index distinct vector spaces so that a covariant index in the ith position must be contracted with some contravariant index in the ith position.
- $\mathcal{B}$ is closed, representing that every index is contracted.

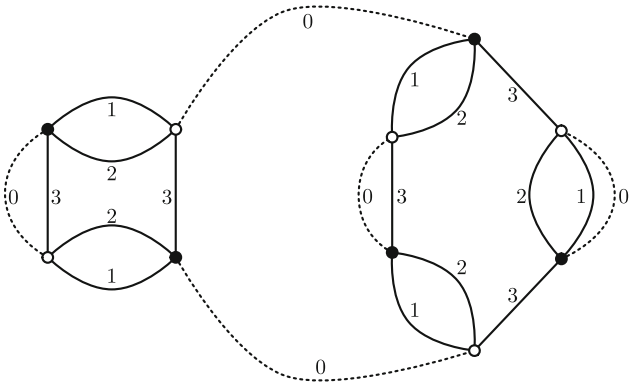

FIGURE 12. A Wick contraction of two trace invariants (for $D = 3$). The contraction of each $(T,\overline{T})$ pair is represented by a *dashed line* of color 0

When facing such a quantity, the standard procedure is to expand it in a Taylor series with respect to the coupling constants $t_{\mathcal{B}}$ and to evaluate the resulting Gaussian integrals in terms of Wick contractions. It transpires that the Feynman graphs $\mathcal{G}$ contributing to $E(\{t_{\mathcal{B}}\})$ are none other than connected closed $(D+1)$-coloured graphs with weight

$$A_{\mathcal{G}} = \frac{(-1)^{|\rho|}}{\mathrm{sym}(\mathcal{G})}\Big(\prod_{\rho} t_{\mathcal{B}_{(\rho)}}\Big) N^{-\frac{2}{(D-1)!}\omega(\mathcal{G})}, \tag{78}$$

where $\mathrm{sym}(\mathcal{G})$ is a symmetry factor, $\mathcal{B}_{(\rho)}$ runs over the subgraphs with colours $\{1,\dots D\}$ of $\mathcal{G}$ and $\omega(\mathcal{G})$ is the degree of $\mathcal{G}$. A few more words of explanation are most definitely in order here. The graphs $\mathcal{G} \in \Gamma^{(D+1)}$ arise in the following manner: one knows that a given term in the Taylor expansion is a product of trace invariants upon which one performs Wick contractions. For such a term, one indexes these trace invariants by $\rho \in \{1,\dots,\rho^{\max}\}$, that is, we index their associated D-coloured graphs $\mathcal{B}_{(\rho)}$. A single Wick contraction pairs a tensor T, lying somewhere in the product, with a tensor $\overline{T}$ lying somewhere else. One represents such a contraction by joining the black vertex representing T to the white vertex representing $\overline{T}$ with a line of colour 0. Thus, a complete set of Wick contractions results in a closed connected (as one is dealing with the free energy) $(D+1)$-coloured graph. A particular Wick contraction is drawn in Fig. 12.

It requires a bit more work to reconstruct the amplitude explicitly, see [57]. Importantly, $\omega(\mathcal{G})$ is a non-negative integer and so one can order the terms in the Taylor expansion of Eq. (77) according to their power of $1/N$. Quite evidently, therefore, one has a *1/N*-expansion.

In the large-N limit only one subclass of graphs survives, containing those graphs with $\omega(\mathcal{G}) = 0$. In [28], it was shown that the only graphs of degree zero are the melonic graphs. Moreover, at leading order in $1/N$ the graphs contributing to the two point function are the rooted melonic graphs.

Appendix B. Proof of Lemma 1

Lemma. *One has*

$$S_q^n := \sum_{n_1,\dots n_q\geq 1}^{n_1+\cdots n_q=n} \frac{n!}{n_1!\dots n_q!} = \sum_{0\leq r\leq q} (-1)^{q-r}\binom{q}{r} r^n.$$

Proof. Note that

$$q^n = \sum_{n_1,\dots n_q\geq 0}^{n_1+\cdots n_q=n} \frac{n!}{n_1!\dots n_q!} = \sum_{r=1}^{q}\binom{q}{r}\sum_{n_1,\dots n_r\geq 1}^{n_1+\cdots n_r=n} \frac{n!}{n_1!\dots n_r!} = \sum_{r=1}^{q}\binom{q}{r} S_r^n. \tag{79}$$

Let us define L as a lower triangular $q\times q$ matrix with non-zero entries: $L_{rs} = \binom{r}{s}$ for $q\geq r\geq s\geq 1$. Then, the S_q^n given in Eq. (7) provide the solution to the system of equations:

$$r^n = \sum_s L_{rs} S_s^n, \quad \text{for all } r \text{ such that } 1\leq r\leq q. \tag{80}$$

We shall show that the lower triangular $q\times q$ matrix P, with entries

$$P_{rs} = (-1)^{r-s}\binom{r}{s}, \quad \text{for} \quad q\geq r\geq s\geq 1, \tag{81}$$

is the inverse of L. The key is to consider the following two series expansions:

$$(1+x)^r = \sum_{s=0}^{r}\binom{r}{s}x^s, \qquad \frac{x^t}{(1+x)^{t+1}} = \sum_{s\geq t}\binom{s}{t}(-1)^{s-t}x^s. \tag{82}$$

Taking their Cauchy product, one finds

$$(1+x)^{r-t-1}x^t = (1+x)^r\frac{x^t}{(1+x)^{t+1}} = \sum_{n\geq t} x^n\left[\sum_{\substack{t\leq s\leq n\\ t-s\leq r}}\binom{r}{n-s}(-1)^{s-t}\binom{s}{t}\right]. \tag{83}$$

However, from a direct expansion of the left-hand side of Eq. (83), one can see that for $t<r$, the coefficient of x^r in $(1+x)^{r-t-1}x^t$ is exactly 0. Hence

$$\forall\, t<r, \qquad \sum_{t\leq s\leq r}\binom{r}{r-s}(-1)^{s-t}\binom{s}{t} = 0. \tag{84}$$

As a result, one has the following two relationships:

$$\sum_s L_{rs}P_{st} = \sum_{t\leq s\leq r}\binom{r}{s}(-1)^{s-t}\binom{s}{t} = \left\{\begin{array}{ll} 0 & r<t\\ 1 & \text{for } r=t\\ 0 & r>t\end{array}\right\} = \delta_{rt} \tag{85}$$

$$\sum_r P_{rs}L_{st} = \sum_{t\leq s\leq r}(-1)^{r-s}\binom{r}{s}\binom{s}{t} = (-1)^{r+t}\sum_s L_{rs}P_{st}. \tag{86}$$

Thus, one finds that as $q\times q$ matrices, L and P are inverse and the claim follows. □

Appendix C. Explanation of Theorem 1 in Section 3

In Sect. 3, we provided the statement

Theorem. *Under the uniform distribution, the family of melonic D-balls converges in the Gromov–Hausdorff topology on compact metric spaces to the continuum random tree:*

$$\left(m_n, \frac{d_{m_n}}{\Lambda_\Delta \sqrt{(D+1)n/D}}\right) \xrightarrow[n\to\infty]{} (\mathcal{T}_{2e}, d_{2e}). \tag{87}$$

As stated earlier, an exhaustive proof along the lines of [49] would inevitably be lengthy. Here, we shall give a very brief sketch. From the discussion at the end of Sect. 4, the proof of this result boiled down to showing that

$$\left(\frac{d_{m_n}(s_1 n, s_2 n)}{\Lambda_\Delta \sqrt{(D+1)n/D}}\right)_{(s_1,s_2)\in[0,1]^{\times 2}} \xrightarrow[n\to\infty]{} \big(d_{2e}(s_1,s_2)\big)_{(s_1,s_2)\in[0,1]^{\times 2}}.$$

In fact, the proof of this point is not so direct. Rather, it rests on the following seminal result of Aldous [54]:

Under the uniform distribution, the family of trees associated with a critical Galton–Watson process with variance σ converges in the Gromov–Hausdorff topology on compact metric spaces to the continuum random tree:

$$\left(T_n, \frac{d_{T_n}}{\sqrt{n/\sigma}}\right) \xrightarrow[n\to\infty]{} (\mathcal{T}_{2e}, d_{2e}). \tag{88}$$

A Galton–Watson process is a stochastic process $\{Z_k\}$, evolving according to $Z_{k+1} = \sum_{i=1}^{Z_k} \xi_j^{(k)}$ where the $\xi_j^{(k)}$ are random variables, taking values in $\mathbb{Z}_+$, independently and identically distributed according some distribution μ. Colloquially, k is the generation number, Z_k is the number of offspring in the kth generation, while μ is the offspring distribution, so that μ_j is the probability that any member has j children. A process is critical if its mean is one: $\sum_{j=0}^{\infty} j\,\mu_j = 1$. The variance of the distribution is $\sigma = \sum_{j=0}^{\infty} j(j-1)\,\mu_j$. Obviously, if $Z_0 = 1$, the process has one initiator and any instance of the process can be mapped to a tree.

A Galton–Watson tree, T, is a tree generated by this process. For the theorem above, one is interested in Galton–Watson trees conditioned to have a total of n progeny, that is, trees T_n with n vertices. Alternatively, critical Galton–Watson trees can be obtained as simply generated trees. The offspring distribution induces a distribution for T_n on the set of all (plane) trees with n vertices, denoted $\mathcal{T}_n$. Specifically, we associate to every tree a weight $\Pi_\mu(T_n) := \prod_{v\in T_n} \mu_{k_v}$, where v are the vertices of T_n and k_v the number of offspring of v. One then picks at random plane trees with probabilities proportional to this weight.

$$P(T_n) = \frac{1}{\sum_{T_n\in\mathcal{T}_n} \Pi_\mu(T_n)} \Pi_\mu(T_n). \tag{89}$$

The strategy is to show that the family of melonic D-balls (seen as random metric spaces under the uniform distribution) correspond to some family of Galton–Watson trees (seen as random metric spaces under the $P(T_n)$ distribution).

The main flow of the argument has three parts:

Part 1. From melonic D-balls to Galton–Watson trees: Fortunately, one knows already that melonic D-balls are in correspondence with coloured rooted $(D+1)$-ary trees. The aim is to show that these are generated by a critical Galton–Watson process. The appropriate offspring distribution is: $\mu_0 = D/(D+1), \mu_{D+1} = 1/(D+1)$, with the rest zero. Such a tree with a total of $(D+1)n+1$ vertices (n internal and $Dn+1$ boundary) is denoted by $T_{(D+1)n+1}$.

Part 2. Distributions: The weight Π_μ on such trees satisfies $\Pi_\mu(T_{(D+1)n+1}) = D^{Dn+1}/(D+1)^{(D+1)n+1}$. Thus, it is constant across $\mathcal{T}_{(D+1)n+1}$, the set of coloured rooted $(D+1)$-ary trees with $(D+1)n+1$ vertices, and corresponds to the uniform distribution:

$$P(T_{(D+1)n+1}) = \frac{1}{C_n^{(D+1)}} \ , \text{ where } C_n^{(D+1)} = \frac{1}{(D+1)n+1}\binom{(D+1)n+1}{n}. \tag{90}$$

$C_n^{(D+1)}$ counts the number of elements in the set $\mathcal{T}_{(D+1)n+1}$.

Part 3. Metrics: The problem becomes yet more nuanced when one moves to the metric spaces associated with the melonic D-balls. The metric space $(m_n, d_{m_n}/\Lambda_\Delta\sqrt{(D+1)n/D})$ takes into account the n internal vertices of M_n only. These are in correspondence with the internal vertices of some element of $\mathcal{T}_{(D+1)n+1}$, say $T_{(D+1)n+1}$. One denotes the defoliated tree corresponding to $T_{(D+1)n+1}$ by T_n. One can cut through a lot of red tape by noticing that these defoliated trees are also generated by their own critical Galton–Watson process with binomial offspring distribution on the first $D+2$ weights: $\mu_j = \binom{D+1}{j} D^{D+1-j}/(D+1)^{D+1}$, for $0 \leq j \leq D+1$ and the rest of the weights zero. This is critical with variance $\sigma = D/(D+1)$. Thus the appropriate result to quote is that

Under the uniform distribution, the family of trees associated with a critical Galton–Watson process with variance σ converges in the Gromov–Hausdorff topology on compact metric spaces to the continuum random tree:

$$\left(T_n, \frac{d_{T_n}}{\sqrt{(D+1)n/D}}\right) \xrightarrow[n\to\infty]{} (\mathcal{T}_{2e}, d_{2e}), \tag{91}$$

where d_{T_n} is the tree distance in the defoliated $(D+1)$-ary tree T_n. The vertices of T_n have a lexicographical order $r \in \{0, \ldots, n-1\}$ generated from their associated words. Thus, for two vertices r_1 and r_2 (in correspondence with two vertices r_1, r_2 in the melonic D-ball), $d_{T_n}(r_1, r_2)$ is the tree distance between r_1 and r_2 in the tree T_n.

One extends d_{T_n} to a continuous metric by interpolating between the integer points in the same fashion as for d_{m_n}. As a result of this (and so-called tightness of this family of rescaled tree metrics), one has

$$\left(\frac{d_{T_n}(s_1 n, s_2 n)}{\sqrt{(D+1)n/D}}\right)_{(s_1,s_2)\in[0,1]^{\times 2}} \xrightarrow[n\to\infty]{} \big(d_{2e}(s_1,s_2)\big)_{(s_1,s_2)\in[0,1]^{\times 2}}. \tag{92}$$

Therefore, the final point is to show the following convergence of rescaled metrics:

$$\left|\frac{d_{m_n}(\lfloor s_1 n\rfloor, \lfloor s_2 n\rfloor)}{\Lambda_\Delta\sqrt{(D+1)n/D}} - \frac{d_{T_n}(\lfloor s_1 n\rfloor, \lfloor s_2 n\rfloor)}{\sqrt{(D+1)n/D}}\right| \xrightarrow[n\to\infty]{(p)} 0 \tag{93}$$

for all $(s_1, s_2) \in [0,1]^{\times 2}$. (p) indicates that the results holds with probability close to 1. The route to this result is far from short. The (very) rough gist of the argument goes as follows. Consider some fixed pair (s_1, s_2) with $s_1 < s_2$. Then, for each tree T_n in the sequence, one can decompose the paths from the root vertex to $w(\lfloor s_1 n\rfloor)$ and $w(\lfloor s_2 n\rfloor)$ as

$$w(\lfloor s_1 n\rfloor) = w_{\text{trunk}}\, l_0\, l_{\text{branch}} \quad \text{and} \quad w(\lfloor s_2 n\rfloor) = w_{\text{trunk}}\, r_0\, r_{\text{branch}}, \tag{94}$$

where w_{trunk} is the word corresponding to the common part of their ancestry, l_0, r_0 are their respective first letters after they diverge and $l_{\text{branch}}, r_{\text{branch}}$ are their respective remaining letters.[4]

One now considers the following sequences of random variables:

$$X_n = (w_{\text{trunk}}, l_{\text{branch}}, r_{\text{branch}}, l_0, r_0),$$

and

$$\widetilde{X}_n = (\widetilde{w}_{\text{trunk}}, \widetilde{l}_{\text{branch}}, \widetilde{r}_{\text{branch}}, \widetilde{l}_0, \widetilde{r}_0), \tag{95}$$

where all the components are independent random variables in their own right and the tilde indicates that the variables are drawn conditionally on some values for the word-lengths $|w_{\text{trunk}}|, |l_{\text{branch}}|$ and $|r_{\text{branch}}|$ at each n. The first three in each set are drawn from W_{D+1}, while the final pair are drawn from $I_{D+1} = \{(a,b) : a, b \in \{0,\dots,D\} \text{ and } a < b\}$. Furthermore, consider the following sequences of functions of these variables:

$$\begin{aligned} g_n(X_n) &= \sqrt{\frac{D}{(D+1)n}}\big(|l_{\text{branch}}|, |r_{\text{branch}}|, \Lambda(l_{\text{branch}}), \Lambda(r_{\text{branch}})\big) \\ g_n(\widetilde{X}_n) &= \sqrt{\frac{D}{(D+1)n}}\big(|\widetilde{l}_{\text{branch}}|, |\widetilde{r}_{\text{branch}}|, \Lambda(\widetilde{l}_{\text{branch}}), \Lambda(\widetilde{r}_{\text{branch}})\big). \end{aligned} \tag{96}$$

For a moment, assume that one can show that as $n \to \infty, g_n(X_n) \to (a_{s_1}, a_{s_2}, \Lambda_\Delta a_{s_1}, \Lambda_\Delta a_{s_2})$ for some a_{s_1} and a_{s_2}. Recalling Eq. (22) and

[4] The notation is meant to be somewhat suggestive. If $s_1 < s_2$, the lexicographical order on the vertices ensures that $w(\lfloor s_1 n\rfloor)$ occurs to the left of $w(\lfloor s_2 n\rfloor)$ in the plane drawing of the tree. Hence, l_{branch} and r_{branch} denote left branch and right branch, respectively.

taking into account that $|\Lambda(l_0 l_{\text{branch}}) - \Lambda(l_{\text{branch}})| \leq 1$, the following inequalities hold:

$$\begin{vmatrix} d_{T_n}(\lfloor s_1 n \rfloor, \lfloor s_2 n \rfloor) - |l_{\text{branch}}| - |r_{\text{branch}}| \end{vmatrix} \leq 2 \\ \begin{vmatrix} d_{m_n}(\lfloor s_1 n \rfloor, \lfloor s_2 n \rfloor) | - \Lambda(l_{\text{branch}}) - \Lambda(r_{\text{branch}}) \end{vmatrix} \leq 8. \tag{97}$$

These imply that $\sqrt{\frac{D}{(D+1)n}} |\Lambda_\Delta d_{T_n}(\lfloor s_1 n \rfloor, \lfloor s_2 n \rfloor) - d_{m_n}(\lfloor s_1 n \rfloor, \lfloor s_2 n \rfloor)| \xrightarrow[n\to\infty]{(p)} 0$ and so the stated convergence Eq. (93) holds.

There is, however, one final catch. One first shows only $g_n(\widetilde{X}_n) \to (a_{s_1}, a_{s_2}, \Lambda_\Delta a_{s_1}, \Lambda_\Delta a_{s_2})$ for some a_{s_1} and a_{s_2}, rather than $g_n(X_n)$. By [55] (Lemma 16 therein), one implies the other if the distributions governing X_n and $\widetilde{X}_n$ converge as $n \to \infty$. This element of the argument is proved in detail in [49] (Lemmas 35 and 36 therein).

Appendix D. Proof of Lemma 4

In order to prove that

$$H^{(n_1,\dots n_p)}(z) := \sum_{\mathcal{M}} z^{N_{\mathcal{M}}} \, h_{\mathcal{M}}^{(n_1)} h_{\mathcal{M}}^{(n_2)} \dots h_{\mathcal{M}}^{(n_p)} \sim u^{\frac{1}{2} - p - \frac{3}{2}(n_1+n_2+\dots+n_p)}, \\ \text{as} \quad z \uparrow z_0, \tag{98}$$

with $u = 1 - z/z_0$, one uses an inductive argument.

To proceed, one requires a set of initial cases that are explicitly shown to satisfy the claim. Here, these turn out to be given by the set of $H^{(0,\dots,0)}$; in other words, for any p, where $n_i = 0$ for all $1 \leq i \leq p$. It emerges that

$$H^{(0,\dots 0)}(z) = \sum_{\mathcal{M}} z^{N_{\mathcal{M}}} \left[h_{\mathcal{M}}^{(0)}\right]^p = \sum_N [(D+1)N+1]^p \, \frac{1}{DN+1} \binom{DN+1}{N} z^N \\ \sim \sum_N \left(\frac{z}{z_0}\right)^N N^{p-3/2} \sim u^{1/2-p}, \tag{99}$$

since for a generic melon, $\mathcal{M}$, with $2N$ vertices $h_{\mathcal{M}}^{(0)} = (D+1)N + 1$. One has furthermore that

$$H^{()} = \sum_{\mathcal{M}} z^{N_{\mathcal{M}}} = \sum_N \frac{1}{DN+1} \binom{DN+1}{N} z^N \sim \text{constant} + u^{1/2}, \\ [H^{()}]^k \sim \text{constant} + u^{1/2}, \\ H^{()} = 1 + z(H^{()})^D \implies \left(1 - Dz[H^{()}]^{D-1}\right) = \frac{(H^{()})^D}{[H^{()}]'} \sim u^{1/2}. \tag{100}$$

To help with the inductive process, one expands $h_{\mathcal{M}}^{(n)}$ as a function of its sub-melons $\mathcal{M}^i$. The label r refers to the number of derivatives that act on the denominator, which yields

$$
\begin{aligned}
h^{(n)}_{\mathcal{M}} &= \frac{\partial^n}{\partial y^n}\left(\frac{1+y+\sum_i h_{\mathcal{M}^i}(y)}{1+(1-y)\sum_i h_{\mathcal{M}^i}(y)}\right)\Bigg|_{y=1} \\
&= 2\delta_{n,0}+\delta_{n,1}+\sum_i h^{(n)}_{\mathcal{M}^i}+\sum_{r=1}^{n}\binom{n}{r}\partial^r\Big[\frac{1}{1+(1-y)\sum_i h_{\mathcal{M}^i}(y)}\Big] \\
&\quad\times\partial^{n-r}\Big[1+y+\sum_i h_{\mathcal{M}^i}(y)\Big] \\
&= 2\delta_{n,0}+\delta_{n,1}+\sum_i h^{(n)}_{\mathcal{M}^i}+2\sum_{s=1}^{n}\sum_{\substack{a_1\ldots a_n \\ [0.05cm]\sum a_j=s\,;\,\sum j a_j=n}} \\
&\quad\times d_{(n,s,a_j)}\prod_{j=1}^{n}\Big[j\sum_i h^{(j-1)}_{\mathcal{M}^i}\Big]^{a_j} \\
&\quad+\sum_{s=1}^{n-1}\sum_{\substack{a_1\ldots a_{n-1} \\ [0.05cm]\sum a_j=s\,;\,\sum j a_j=n-1}} d_{(n-1,s,a_j)}\prod_{j=1}^{n-1}\Big[j\sum_i h^{(j-1)}_{\mathcal{M}^i}\Big]^{a_j} \\
&\quad+\sum_{r=1}^{n}\sum_i h^{(n-r)}_{\mathcal{M}^i}\sum_{s=1}^{r}\sum_{\substack{a_1\ldots a_r \\ [0.05cm]\sum a_j=s\,;\,\sum j a_j=r}} d_{(r,s,a_j)}\prod_{j=1}^{r}\Big[j\sum_i h^{(j-1)}_{\mathcal{M}^i}\Big]^{a_j},
\end{aligned}
\tag{101}
$$

where

$$
d_{(r,s,a_j)}=\binom{n}{r}\frac{r!}{(1!)^{a_1}\ldots[r!]^{a_r}a_1!\ldots a_r!}(-1)^{s+1}s! \tag{102}
$$

and Eq. (67) has been used to obtain the final form.

While the stage has been set to invoke the inductive hypothesis, it is beneficial to first tackle a simple example. Actually, this transpires that it is remarkable indicative of the general argument. The case in question occurs at $p=1$, with $n_1=1$. Evaluating the recursive Eq. (101) in this case, one finds

$$
h^{(1)}_{\mathcal{M}}=1+\sum_i h^{(1)}_{\mathcal{M}^i}+2\sum_i h^{(0)}_{\mathcal{M}^i}+\left[\sum_i h^{(0)}_{\mathcal{M}^i}\right]^2, \tag{103}
$$

which leads to the following equation for $H^{(1)}$ (recall that $N=\sum_i N_i+1$):

$$
\begin{aligned}
H^{(1)}(1-zD[H^{()}]^{D-1}) &= H^{()}+2zDH^{(0)}[H^{()}]^{D-1} \\
&\quad+zD(D-1)H^{(0)}H^{(0)}[H^{()}]^{D-2} \\
&\quad+zDH^{(0,0)}[H^{()}]^{D-1},
\end{aligned}
\tag{104}
$$

with the use of the helpful remark that

$$
\sum_{\mathcal{M}} z^{N_{\mathcal{M}}}h^{(n)}_{\mathcal{M}^i}=zH^{(n)}[H^{()}]^{D-1}. \tag{105}
$$

The most singular term is the one involving $H^{(0,0)}$; thus one finds that the behaviour of $H^{(1)}$ is

$$H^{(1)} \sim u^{-2}, \tag{106}$$

which is in agreement with the claim. More importantly, one should note that the relation Eq. (104) allows one to express $H^{(1)}$ in terms of Hs with lower valued indices, although the number of indices may increase. Obviously, any inductive argument requires that one put an order on the set of $H^{(n_1,\dots,n_p)}$. The above example should make one aware that this ordering is subtle.

(As a brief aside, one notes that Eq. (104) is slightly different from the analogous equation given in [48] for the case of branched polymers. Obviously, appearances of D are to be expected. However, one may be slightly puzzled as to the presence of factors of z. There is a simple reason for this occurrence. In the case of binary branched polymers (trees), the terms are labelled according to their total number of vertices R. This satisfies $R = R_1 + R_2$, where the R_i are the two sub-branches. In the case of rooted melonic graphs, the formula for N is: $N = 1 + \sum_i N_i$, as stated above Eq. (61). This extra 1 on the right-hand side leads to the presence of the z-factors.)

Returning to the main theme, the aim now is to put an appropriate order relation on the possible lists of indices (non-negative integers) S of $H^{(S)}$. Let us start by ordering the elements of S in decreasing order from left to right, that is, $S(i) \geq S(i+1)$ if $S(i)$ denotes the i'th element of S. Furthermore, one denotes by $|S|$ the number of entries in the list S. One orders the lists in lexicographical order, that is, $S_a > S_b$ if one of the three following statements holds:

- $S_a(1) > S_b(1)$.
- $S_a(i) = S_b(i)$ for $1 \leq i < i_0$ and $S_a(i_0) > S_b(i_0)$.
- $S_a(i) = S_b(i)$ for $1 \leq i \leq |S_b|$ and $|S_a| > |S_b|$.

Note that $>$ is a total order relation: for any $S_a \neq S_b$, one either has $S_a > S_b$ or $S_b > S_a$. One states $S_a \supset S_b$ if all the elements in the list S_b together with their multiplicities are also elements in the list S_a. If $S_a \supset S_b$ and $|S_a| > |S_b|$ then $S_a > S_b$.

One uses this order relation in the following way. Consider an abridged form of Eq. (101)

$$h_{\mathcal{M}}^{(n)} = \sum_i h_{\mathcal{M}^i}^{(n)} + T(n-1), \tag{107}$$

where $T(n-1)$ contains the remaining terms, which by design possess derivatives of order at most $n-1$. Let $S = \{\underbrace{n,\dots,n}_{q}, n_1, \dots, n_{p_S}\}$, with $n > n_1 \geq n_2 \cdots \geq n_{p_S}$. One may write any H as

$$H^{(S)} = \sum_{\mathcal{M}} z^{N_{\mathcal{M}}} \left[h_{\mathcal{M}}^{(n)}\right]^q \prod_j h_{\mathcal{M}}^{(n_j)}$$
$$= \sum_{\mathcal{M}} z^{N_{\mathcal{M}}} \left(\sum_i h_{\mathcal{M}^i}^{(n)} + T(n-1)\right)^q \prod_j \left(\sum_i h_{\mathcal{M}^i}^{(n_j)} + T(n_j - 1)\right), \tag{108}$$

The generic form of a term on the right-hand side of Eq. (108) evaluates to

$$\prod_i H^{(S_i)}, \tag{109}$$

where S_i denotes the set of indices pertaining to the sub-melon $\mathcal{M}^i$ in the product. There are a number of possibilities:

There is a term for each fixed i corresponding to choosing $h_{\mathcal{M}^i}^{(\dots)}$ in all the terms. It has $S_i = S$ and $S_j = \emptyset$ for all $j \neq i$. These terms are brought over to the left-hand side of Eq. (108).

The rest of the terms may be divided in several classes:

- Terms with no factor T. They subdivide as
  - no single set S_i possesses all q indices of value n. Hence $S_i < S$ for all i.
  - a single set S_i possesses all q indices of value n. But then S_i must have less than p_S elements drawn from $\{n_1, \dots, n_{p_S}\}$. One has $S_j < S$ for $j \neq i$ and $S \supset S_i, |S| > |S_i|$ hence $S_i < S$.
- There is at least one factor of $T(n-1)$ and any number of factors of $T(n_j - 1)$ for the various j. In this case, any given S_i contains fewer than q indices of value n, hence $S_i < S$ for all i.
- There is at least one factor of some $T(n_j - 1)$ but no factors of $T(n-1)$. In this case, a given S_i may contain the index n up to q times, at most $p_S - 1$ indices $\{n_{i_1}, \dots n_{i_k}\}$ drawn from $\{n_1, \dots, n_{p_S}\}$ with $k \leq p_S - 1$ and the rest drawn from integers strictly smaller that

$$\max_{n \in \{n_1, \dots, n_{p_S}\} \setminus \{n_{i_1}, \dots n_{i_k}\}} n; \tag{110}$$

  hence $S_i < S$.

One now proceeds to a more refined analysis of the leading divergent behaviour of the various terms involved in Eq. (108). One first associates a number, called the naïve index d_0, with every $h_{\mathcal{M}}^{(n)}$:

$$d_0\left(h_{\mathcal{M}}^{(n)}\right) := -1 - \frac{3}{2}n, \tag{111}$$

The definition readily extends to products, $d_0\left(\prod_j h_{\mathcal{M}^j}^{(n_j)}\right) = \sum_j d_0\left(h_{\mathcal{M}^j}^{(n_j)}\right)$. It is convenient to regroup the terms in Eq. (101) as

$$h_{\mathcal{M}}^{(n)} = \sum_i h_{\mathcal{M}^i}^{(n)} + \sum_i \sum_{r=1}^{n} h_{\mathcal{M}^i}^{(n-r)} \binom{n}{r} r h_{\mathcal{M}^i}^{(r-1)} + T', \tag{112}$$

where the terms in T' have either (i) naïve index at least $-1-\frac{3}{2}n+\frac{3}{2}$ or (ii) naïve index $-1-\frac{3}{2}n+\frac{1}{2}$ but possesses at least two entries $h^{(\dots)}_{\mathcal{M}^i}$ and $h^{(\dots)}_{\mathcal{M}^j}$ corresponding to two distinct melons. It is time to proceed to the inductive argument.

Inductive hypothesis: For all $R=\{r_1,\dots r_t\}<S$ the actual degree of divergence d_a of $H^{(R)}$ (that is, $H^{(R)}\sim u^{d_a}$) is

$$d_a\big(H^{(R)}\big)=\frac{1}{2}+d_0\left(\prod_{j=1}^{t}h^{(r_j)}_{\mathcal{M}}\right). \tag{113}$$

Inductive step: Assume that the claim holds for all sets $R<S=\{n_1,\dots,n_p\}$. First, one expands $H^{(S)}$:

$$H^{(S)}=\sum_{\mathcal{M}}z^{N_{\mathcal{M}}}\prod_j\left(\sum_i h^{(n_j)}_{\mathcal{M}^i}+\sum_i\sum_{r=1}^{n_j}h^{(n_j-r)}_{\mathcal{M}^i}\binom{n_j}{r}rh^{(r-1)}_{\mathcal{M}^i}+T'\right) \tag{114}$$

Any term on the right-hand side of Eq. (114) has the generic form Eq. (109). All the $S_i<S$, so that one can invoke the inductive hypothesis Eq. (113). The actual degree of divergence of this product is related to the naïve index of its corresponding constituents as

$$d_a\left(\prod_i H^{(S_i)}\right)=\frac{k}{2}+d_0\left(\text{constituents of }\prod_i H^{(S_i)}\right)$$
$$\text{if } k \text{ out of } D \text{ sets } S_i \text{ are non-empty.} \tag{115}$$

This apparent anomaly stems from the fact that if a set S_i is empty, the contribution $H^{()}$ scales like u^0 rather than $u^{1/2}$. This shows that one can discard almost all terms in the sum on the right-hand side: in fact, only three classes of term survive:

$$\begin{aligned}&H^{(n_1,\dots,n_p)}\\&=\sum_{\mathcal{M}}z^{N_{\mathcal{M}}}\Bigg[\sum_i\prod_j h^{(n_j)}_{\mathcal{M}^i}+\sum_{i_1,\,i_2}\ \prod_{j_1\in J_1,\,j_2\in J_2}h^{(n_{j_1})}_{\mathcal{M}^{i_1}}h^{(n_{j_2})}_{\mathcal{M}^{i_2}}\\&\qquad\qquad[0.05cm]i_1\neq i_2\ [0.05cm]J_1\cup J_2=\{n_1,\dots,n_p\}\\&\qquad+\sum_i\sum_j\left(\sum_{r=1}^{n_j}\binom{n_j}{r}rh^{(r-1)}_{\mathcal{M}^i}h^{(n_j-r)}_{\mathcal{M}^i}\prod_{k\neq j}h^{(n_k)}_{\mathcal{M}^i}\right)\Bigg].\end{aligned} \tag{116}$$

The first term survives because all indices n_j are attached to a single sub-melon $\mathcal{M}^i$. Thus, it generates a term containing a factor of $H^{(n_1,\dots,n_p)}$. As a result, it is transferred to the left-hand side (where it belongs).

The second term has naïve index: $d_0=-p-\frac{3}{2}\sum_j n_j$. On top of that, all indices are attached to exactly two sub-melons $\mathcal{M}^{i_1}$ and $\mathcal{M}^{i_2}$. Thus, after summation, it leads to terms with exactly two non-empty sets, S_{i_1} and S_{i_2}.

From Eq. (115), the actual degree of divergence of these terms is $d_a = 1 + d_0 = 1 - p - \frac{3}{2}\sum_j n_j$.

The third term has naïve index: $d_0 = -p - \frac{3}{2}\sum_j n_j + \frac{1}{2}$. As all indices are attached to a single sub-melon it leads after resummation to a term with actual degree of divergence $d_a = \frac{1}{2} - p - \frac{3}{2}\sum_j n_j + \frac{1}{2}$; hence it contributes also to the leading order divergence.

All the terms one eliminated from Eq. (116) fall into one of the following categories:

- Terms involving at least three different melons $h^{(n_{j_1})}_{\mathcal{M}^{i_1}}, h^{(n_{j_2})}_{\mathcal{M}^{i_2}}$ and $h^{(n_{j_3})}_{\mathcal{M}^{i_3}}$. They have naïve index at least $-p - \frac{3}{2}\sum_j n_j$. Hence, their actual degree of divergence is at least $\frac{3}{2} - p - \frac{3}{2}\sum_j n_j$.
- Terms involving a $\sum_{r=1}^{n_j}\binom{n_j}{r} r h^{(r-1)}_{\mathcal{M}^i} h^{(n_j-r)}_{\mathcal{M}^i}$ and a $h^{(n_{j_1})}_{\mathcal{M}^{i_1}}$ for $i_1 \neq i$. They have naïve index at least $-p - \frac{3}{2}\sum_j n_j + \frac{1}{2}$ and involve at least two distinct melons. Hence, their actual degree of divergence is at least $1 - p - \frac{3}{2}\sum_j n_j + \frac{1}{2}$.
- Terms involving at least two factors $\sum_{r=1}^{n_j}\binom{n_j}{r} r h^{(r-1)}_{\mathcal{M}^i} h^{(n_j-r)}_{\mathcal{M}^i}$. They have naïve index at least $-p - \frac{3}{2}\sum_j n_j + 1$. Hence, their actual degree of divergence is at least $\frac{1}{2} - p - \frac{3}{2}\sum_j n_j + 1$.
- Terms involving T'. They have either (i) naïve index at least $-p - \frac{3}{2}\sum_j n_j + \frac{3}{2}$. Hence, their actual degree of divergence is at least $\frac{1}{2} - p - \frac{3}{2}\sum_j n_j + \frac{3}{2}$, or (ii) naïve index $-p - \frac{3}{2}\sum_j n_j + \frac{1}{2}$ but involve at least two distinct melons. Hence, their actual degree of divergence is at least $1 - p - \frac{3}{2}\sum_j n_j + \frac{1}{2}$.

Explicit resummation gives

$$\begin{aligned} & sH^{(n_1,\dots,n_p)}\Big(1 - zD\big[H^{()}\big]^{D-1}\Big) \\ & \quad = zD(D-1)\big[H^{()}\big]^{D-2} \sum_{\substack{S_1\neq\emptyset,\, S_2\neq\emptyset \\ S_1\cup S_2 = S\ S_1\cap S_2=\emptyset}} H^{(S_1)}H^{(S_2)} \\ & \qquad + zD\big[H^{()}\big]^{D-1} \sum_{j;n_j\geq 1}\sum_{r=1}^{n_j}\binom{n_j}{r} r H^{(r-1,n_j-r,S\backslash n_j)}, \end{aligned} \tag{117}$$

where a term has been transferred to the left-hand side as indicated and $S\backslash n_j$ is the set S less the element n_j. Note that the first terms on the right-hand side appears only if a partition on S into two nonempty sublists S_1 and S_2 is exists, that is, $|S| \geq 2$. As shown already, the right-hand side scales like $u^{1-p-\frac{3}{2}\sum_j n_j}$ and using Eq. (100), one has that

$$H^{(n_1,\dots,n_p)} \sim u^{\frac{1}{2}-p-\frac{3}{2}\sum_j n_j}.$$

At this stage, one might like to check that the coefficient of this leading order divergence in Eq. (70) does not magically vanish. To that end, bounds on this coefficient may be extracted from Eq. (117) in an analogous manner to those derived in [48] and these show that it is strictly greater than zero. □

References

[1] Gurau, R., Ryan, J.P.: Colored tensor models—a review. SIGMA **8**, 020 (2012), (arXiv:1109.4812 [hep-th])

[2] Di Francesco, P., Ginsparg, P.H., Zinn-Justin, J.: 2-D gravity and random matrices. Phys. Rep. **254**, 1–133 (1995)

[3] Sasakura, N.: Tensor model for gravity and orientability of manifold. Mod. Phys. Lett. A **6**, 2613 (1991)

[4] Ambjorn, J., Durhuus, B., Jonsson, T.: Three-dimensional simplicial quantum gravity and generalized matrix models. Mod. Phys. Lett. A **6**, 1133 (1991)

[5] Sasakura, N.: Tensor models and 3-ary algebras. J. Math. Phys. **52**, 103510 (2011), (arXiv:1104.1463 [hep-th])

[6] Sasakura, N.: Tensor models and hierarchy of n-ary algebras. Int. J. Mod. Phys. A **26**, 3249 (2011), (arXiv:1104.5312 [hep-th])

[7] Boulatov, D.V.: A model of three-dimensional lattice gravity. Mod. Phys. Lett. A **7**, 1629 (1992), (hep-th/9202074)

[8] Ooguri, H.: Topological lattice models in four-dimensions. Mod. Phys. Lett. A **7**, 2799 (1992), (hep-th/9205090)

[9] De Pietri, R., Petronio, C.: Feynman diagrams of generalized matrix models and the associated manifolds in dimension 4. J. Math. Phys. **41**, 6671 (2000), (gr-qc/0004045)

[10] De Pietri, R., Freidel, L., Krasnov, K., Rovelli, C.: Barrett–Crane model from a Boulatov–Ooguri field theory over a homogeneous space. Nucl. Phys. B **574**, 785 (2000), (hep-th/9907154)

[11] Reisenberger, M.P., Rovelli, C.: Space-time as a Feynman diagram: the connection formulation. Class. Quant. Gravity **18**, 121 (2001), (gr-qc/0002095)

[12] Baratin, A., Oriti, D.: Group field theory with non-commutative metric variables. Phys. Rev. Lett. **105**, 221302 (2010), (arXiv:1002.4723 [hep-th])

[13] Baratin, A., Oriti, D.: Group field theory and simplicial gravity path integrals: a model for Holst–Plebanski gravity. Phys. Rev. D **85**, 044003 (2012), (arXiv:1111.5842 [hep-th])

[14] Rovelli, C.: Quantum Gravity. Cambridge University Press, Cambridge (2004)

[15] Engle, J., Livine, E., Pereira, R., Rovelli,C.: LQG vertex with finite Immirzi parameter. Nucl. Phys. B **799**, 136 (2008), (arXiv:0711.0146 [gr-qc])

[16] Freidel, L., Krasnov, K.: A new spin foam model for 4D Gravity. Class. Quant. Gravity **25**, 125018 (2008), (arXiv:0708.1595 [gr-qc])

[17] Livine, E.R., Speziale, S.: Consistently solving the simplicity constraints for spinfoam quantum gravity. Europhys. Lett. **81**, 50004 (2008), (arXiv:0708.1915 [gr-qc])

[18] Perini, C., Rovelli, C., Speziale, S.: Self-energy and vertex radiative corrections in LQG. Phys. Lett. B **682**, 78 (2009), (arXiv:0810.1714 [gr-qc])

[19] Ben Geloun, J., Gurau, R., Rivasseau, V.: EPRL/FK group field theory. Europhys. Lett. **92**, 60008 (2010), (arXiv:1008.0354 [hep-th])

[20] Krajewski, T., Magnen, J., Rivasseau, V., Tanasa, A., Vitale, P.: Quantum corrections in the group field theory formulation of the EPRL/FK models. Phys. Rev. D **82**, 124069 (2010), (arXiv:1007.3150 [gr-qc])

[21] Riello, A.: Self-energy of the Lorentzian EPRL-FK spin foam model of quantum gravity. Phys. Rev. D **88**, 024011 (2013), (arXiv:1302.1781 [gr-qc])

[22] Gurau, R.: Colored group field theory. Commun. Math. Phys. **304**, 69 (2011), (arXiv:0907.2582 [hep-th])

[23] Gurau, R.: The 1/N expansion of colored tensor models. Annales Henri Poincaré **12**, 829 (2011), (arXiv:1011.2726 [gr-qc])

[24] Gurau, R., Rivasseau, V.: The 1/N expansion of colored tensor models in arbitrary dimension. Europhys. Lett. **95**, 50004 (2011), (arXiv:1101.4182 [gr-qc])

[25] Gurau, R.: The complete 1/N expansion of colored tensor models in arbitrary dimension. Annales Henri Poincaré **13**, 399 (2012), (arXiv:1102.5759 [gr-qc])

[26] Bonzom, V.: New 1/N expansions in random tensor models. JHEP **1306**, 062 (2013), (arXiv:1211.1657 [hep-th])

[27] Dartois, S., Rivasseau, V., Tanasa, A.: The 1/N expansion of multi-orientable random tensor models. (arXiv:1301.1535 [hep-th])

[28] Bonzom, V., Gurau, R., Riello, A., Rivasseau, V.: Critical behavior of colored tensor models in the large N limit. Nucl. Phys. B **853**, 174 (2011), (arXiv:1105.3122 [hep-th])

[29] Bonzom, V., Gurau, R., Rivasseau, V.: The Ising model on random lattices in arbitrary dimensions. Phys. Lett. B **711**, 88 (2012), (arXiv:1108.6269 [hep-th])

[30] Bonzom, V.: Multicritical tensor models and hard dimers on spherical random lattices. Phys. Lett. A **377**, 501 (2013), (arXiv:1201.1931 [hep-th])

[31] Bonzom, V., Erbin, H.: Coupling of hard dimers to dynamical lattices via random tensors. J. Stat. Mech. **1209**, P09009 (2012), (arXiv:1204.3798 [cond-mat.stat-mech])

[32] Benedetti, D., Gurau, R.: Phase transition in dually weighted colored tensor models. Nucl. Phys. B **855**, 420 (2012), (arXiv:1108.5389 [hep-th])

[33] Gurau, R.: A generalization of the Virasoro algebra to arbitrary dimensions. Nucl. Phys. B **852**, 592 (2011), (arXiv:1105.6072 [hep-th])

[34] Gurau, R.: The Schwinger Dyson equations and the algebra of constraints of random tensor models at all orders. Nucl. Phys. B **865**, 133 (2012), (arXiv:1203.4965 [hep-th])

[35] Krajewski, T.: Schwinger-Dyson equations in group field theories of quantum gravity. In: Proceedings of the XXIX international colloquium on group-theoretical methods in physics (GROUP 29), (arXiv:1211.1244 [math-ph])

[36] Bonzom, V.: Revisiting random tensor models at large N via the Schwinger-Dyson equations. JHEP **1303**, 160 (2013), (arXiv:1208.6216 [hep-th])

[37] Gurau, R.: Universality for random tensors. To appear in Annales de l'Institut Henri Poincaré (B) Probabilités et Statistiques, (arXiv:1111.0519 [math.PR])

[38] Ben Geloun, J., Rivasseau, V.: A renormalizable 4-dimensional tensor field theory. Commun. Math. Phys. **318**, 69 (2013), (arXiv:1111.4997 [hep-th])

[39] Ben Geloun, J.: Two and four-loop β-functions of rank 4 renormalizable tensor field theories. Class. Quant. Gravity **29**, 235011 (2012), (arXiv:1205.5513 [hep-th])

[40] Ben Geloun, J.: Asymptotic freedom of rank 4 tensor group field theory. (arXiv:1210.5490 [hep-th])

[41] Carrozza, S., Oriti, D.: Bubbles and jackets: new scaling bounds in topological group field theories. JHEP **1206**, 092 (2012), (arXiv:1203.5082 [hep-th])

[42] Carrozza, S., Oriti, D., Rivasseau, V.: Renormalization of tensorial group field theories: abelian U(1) models in four dimensions. (arXiv:1207.6734 [hep-th])

[43] Ambjorn, J., Durhuus, B., Jonsson, T.: Summing over all genera for d > 1: a toy model. Phys. Lett. B **244**, 403–412 (1990)

[44] Bialas, P., Burda, Z.: Phase transition in fluctuating branched geometry. Phys. Lett. B **384**, 75 (1996), (arXiv:hep-lat/9605020)

[45] Ambjorn, J., Durhuus, B., Frohlich, J.: Diseases of triangulated random surface models, and possible cures. Nucl. Phys. B **257**, 433 (1985)

[46] Ambjorn, J., Durhuus, B., Jonsson, T.: Quantum Geometry. A Statistical Field Theory Approach. University Press, Cambridge (Cambridge Monographs in Mathematical Physics), p. 363 (1997)

[47] Ambjorn, J., Jurkiewicz, J., Loll, R.: Dynamically triangulating Lorentzian quantum gravity. Nucl. Phys. B **610**, 347 (2001), (hep-th/0105267)

[48] Jonsson, T., Wheater, J.F.: The spectral dimension of the branched polymer phase of two-dimensional quantum gravity. Nucl. Phys. B **515**, 549 (1998), (hep-lat/9710024)

[49] Albenque, M., Marckert, J.F.: Some families of increasing planar maps. Electron. J. Probab. **13**(56), 1624–1671 (2008)

[50] Pezzana, M.: Sulla struttura topologica delle varietà compatte. Atti Sem. Mat. Fis. Univ. Modena **23**, 269–277 (1974)

[51] Ferri, M., Gagliardi, C.: Crystallisation moves. Pac. J. Math. **100**, 1 (1982)

[52] Gurau, R.: Lost in translation: topological singularities in group field theory. Class. Quant. Gravity **27**, 235023 (2010), (arXiv:1006.0714 [hep-th])

[53] Ryan, J.P.: Tensor models and embedded Riemann surfaces. Phys. Rev. D **85**, 024010 (2012), (arXiv:1104.5471 [gr-qc])

[54] Aldous, D.: The continuum random tree II: an overview (Proceeding of the Durham symposium on stochastic analysis, 1990). Lond. Math. Soc. Lect. Note Ser. **167**, 23–70 (1991)

[55] Marckert, J.F.: The lineage process in Galton–Watson trees and globally centered discrete snakes. Ann. Appl. Probab. **18**(1), 209–244 (2009)

[56] Durhuus, B., Jonsson, T., Wheater, J.F.: The spectral dimension of generic trees. (math-ph/0607020)

[57] Bonzom, V., Gurau, R., Rivasseau, V.: Random tensor models in the large N limit: uncoloring the colored tensor models. Phys. Rev. D **85**, 084037 (2012), (arXiv:1202.3637 [hep-th])

Razvan Gurau
UMR 7644 École Polytechnique
Centre de Physique Théorique
91128 Palaiseau Cedex, France
e-mail: rgurau@cpht.polytechnique.fr
and
Perimeter Institute for Theoretical Physics
31 Caroline St. N
Waterloo, ON N2L 2Y5, Canada

Melons are Branched Polymers

James P. Ryan
Max Planck Institute for Gravitational Physics (Albert Einstein Institute)
Potsdam, Germany
e-mail: james.ryan@aei.mpg.de

Communicated by Abdelmalek Abdesselam.
Received: February 25, 2013.
Accepted: October 11, 2013.